공학박사학위논문

Modeling, Economic Feasibility Analysis and Monitoring of Fuel Cell System

연료전지 시스템에 대한 모델링, 경제성 분석 및 모니터링에 관한 연구

2012년 8월

서울대학교 대학원

화학생물공학부

정 현 석

Abstract

Modeling, Economic Feasibility Analysis and Monitoring of Fuel Cell System

Hyeonseok Jeong

School of Chemical & Biological Engineering

The Graduate School of Seoul National University

The value of fuel cell technology increases as the concerns for depletion of fossil fuels and environmental problems arise. By-product hydrogen generated in chemical complexes is used as feed for other chemical and refinery processes, as a product for sale as well as fuel for boilers. Therefore, high-grade usage of by-product hydrogen is required under these circumstances. Fuel cells whose technology has grown nearly at the level of commercialization are one way hydrogen can be used, giving it such high value. This thesis has three main purposes, which are economic feasibility analysis for proton exchange membrane

fuel cell (PEMFC) power plant, transport phenomena analysis in PEMFC, improvement of monitoring system for molten carbonate fuel cell (MCFC) power plant, respectively.

A PEMFC power plant is economically assessed as one of the methods for the use of by-product hydrogen. The process model is set to demonstrate the economic feasibility of a fuel cell power plant. An economic profitability standard is calculated for the base case and sensitivity analyses are carried out for key variables. Some cases also consider future plans about support systems and variations in prices. The comparison results among various hydrogen sources indicate that by-product hydrogen from chemical complex has an economic advantage.

In this thesis, transport phenomena in a single cell and a stack are simulated by using both steady-state and dynamic model. A two-dimensional, the steady-state rigorous model is developed to simulate a single cell in PEMFC. The model accounts for gas species transport, electrochemical kinetics, charge distribution, and hydrodynamics. The governing differential equations consist of a free-path flow channel, gas-diffusion layer, and catalyst layers for the anode and cathode sides as well as the polymer electrolyte membrane region. The set of governing equations is solved by a finite volume-based fluid dynamics computational algorithm. The proposed model is validated with the experimental polarization curve. A zero-dimensional dynamic model is developed to simulate the stack behavior in PEMFC. This model is based on the lumped dynamic model but was modified to give a more accurate account of the correlation between performance and water management. To analyze this correlation, the modified model includes

three segments of the entrance region, central region, and exit region. The amount of water transport across the membrane and the change in the current for each segment are calculated. The simulation results are analyzed and compared to the benchmarks from lumped stack results and reference literature. The amount of water at the channel outlet is an important aspect of a system that uses fuel cells in vehicles and that cannot be easily supplied with water.

A univariate alarm system, which has only upper and lower limits, is usually employed to identify abnormal conditions in the 300 kW MCFC power plant. This simple monitoring system is limited for using in an extended monitoring system for fault diagnosis. Therefore, based on principal component analysis (PCA), a heuristic variable selection method for a multivariate monitoring system is presented. To verify the performance of the fault detection, real plant operations data are used. Furthermore, comparison between type 1 and type 2 errors for four different variable groups demonstrates that the developed heuristic method performs well when system faults occur. These monitoring techniques can reduce the number of false alarms occurring on-site at MCFC power plant.

This work can contribute to determine proper modeling level for satisfying various purposes of simulation by providing a plenty of cases. Proposed models can be implemented in other purposes such as efficient design and stable operation.

Keywords: Fuel Cell, Modeling and Simulation, Transport Phenomena, Process Monitoring, Economic assessment

Student ID: 2006-21388

Contents

List of Figures

List of Tables

CHAPTER 1 : Introduction

1.1. Research motivation

Fuel cell systems are the most representative power generation system in renewable energy research. A fuel cell system is an eco-friendly power generation system that converts the chemical energy of hydrogen into electric energy with higher efficiency and lower emission than conventional power generation systems. There are several applications for fuel cells, e.g., portable devices, transportation, and stationary power plants that depend on the power generation capacity and the characteristic of fuel cell.[1-5] The applications of stationary power plant and transportation vehicle are classified by the fuel cell types.[6-10] The types of fuel cells are shown in Table 2-1.

Proton exchange membrane fuel cells (PEMFCs) are candidates for environmentally friendly power generation applications because they have high energy density and are energy efficient.[11] The technologies of Phosphoric acid fuel cell (PAFC) and Molten carbonate fuel cell (MCFC) have grown nearly to the level of commercialization.[12-16] UTC Power, Fuji Electric. FCE, and Ansaldo Fuel cells are the most well-known producers of fuel cells. PEMFC studies are at an intermediate level between the demonstration step and commercialization step. Nuvera, Nedstack, and Ballard produce PEMFC power systems for the world.[17-20] On the other hand, manufacturers of the Solid oxide fuel cell (SOFC) system are supported by governments such as the Solid state energy conversion alliance (SECA).[21-22] Therefore, PAFC, MCFC, and PEMFC are considered commercialized fuel cell systems, which could be installed in the near future.[23-24]

PAFC, External-reforming type MCFC, and PEMFC use hydrogen as fuel theoretically. Since hydrogen has some disadvantages in storage and transportation, most of the commercial fuel cell systems obtain hydrogen by reforming hydrocarbons (NG or ADG etc.).[25-27] The reformer systems are installed in the commercial fuel cell systems. Therefore, the various systems of the fuel cells have to be modified to meet the mass and energy balance so that hydrogen can be used as a fuel in hydrocarbon-fueled fuel cells. Most of the commercial PAFC and MCFC use NG as fuel, and are practically very difficult to modify the system for use of by-product hydrogen. Especially, hydrogen-fueled PAFC is highly expensive in the mass production step. Furthermore, studies on external-reforming type MCFC have focused on reforming hydrocarbon by several research groups.[28-29]

In order to deploy on a commercialization, many obstacles are remained, which are prevention of flooding and hydration, cost reduction, extension of life time, securement of stable operation and so on. In order to solve these problems, proper modeling is needed, which is from first principal based model to statistic black box model.[30] According to determine modeling level, an effort to develop model is varied. Especially, fuel cell system is consists of many phenomena, which are electrochemical reaction, chemical reaction, gas flow. Therefore, modeling and simulation of fuel cell system is good example for purpose oriented modeling.

Table 1-1. Characteristics of fuel cells

	PEMFC	PAFC	MCFC	SOFC
Electrolyte	Ion exchange membrane (solid)	Liquid phosphoric acid (liquid)	Molten carbonate salt (liquid)	Solid metal oxide (solid)
Operating Temperature	0-80℃	130-220℃	650℃	750-1050℃
Efficiency	40-60%	36-45%	50-60%	50-55%
Maximum efficiency (with co-gen)	60%	80%	85%	85%
Stack lifetime (hours)	17250 ~25000	40000 ~80000	20000 ~40000	40000 (15' SECA)
Reaction in Anode	$H_2 + 2e^- \rightarrow 2H^+$		$H_2 + 1/2O_2^{2-} \rightarrow H_2O + 2e^-$	
Reaction in Cathode	$2H^+ + 1/2O_2 + 2e^- \rightarrow H_2O$		$1/2O_2 + 2e^- \rightarrow O_2^{2-}$	

1.2. Research objectives

The objective of this thesis is to propose several kinds of purpose oriented modeling and simulation from first principle based rigorous model to statistical black box model. In order to check validity of investigation for the PEMFC power plant, process model of the PEMFC is developed. For considering technology development, zero-dimensional process model is presented to estimate fuel consumption and system efficiency. For understanding transport phenomena of a single cell and stack in the PEMFC, a steady-state two-dimensional rigorous model and a dynamic 3-segment model are proposed. In order to solve the rigorous model, solving algorithm is developed. A lumped dynamic model is modified to estimate more detail distribution of water amount in the channel and the membrane. To improve monitoring performance of fault detection in the MCFC power plant, statistical model is presented. Heuristic variable selection method is developed for higher accuracy of fault detection. The propose method validates error rate using plant operation data in the MCFC power plant.

1.3. Outline of the thesis

Chapter 1 describes fuel cell and necessity of objective oriented modeling and simulation with an introduction of this study and outline of this thesis. Chapter 2 describes the economic assessment analysis using a PEMFC system model for a power plant fueled by by-product hydrogen with a pressure swing adsorption unit. Chapter 3 describes analysis of transport phenomena in a single cell and a stack of PEMFC. It includes a steady-state and a dynamic simulation with validation using

experimental data. Chapter 4 describes a methodology of monitoring using a statistic model for a MCFC power plant. Further, in this chapter, we suggested variable selection method to improve monitoring performance. It includes validation with operation data from an installed plant. Chapter 5 presents the conclusions and an outline for future works.

CHAPTER 2 : Modeling and Simulation of PEMFC for Economic Feasibility Analysis*

2.1. Introduction

In petrochemical complexes, hydrogen has been produced as a by-product by diverse chemical processes. The high quality by-product hydrogen, which has uniform purity, has several potential uses such as feed for a refinery processes or as a product for sale. Low quality by-product hydrogen, on the other hand, is usually exhausted as fuel for boilers to generate steam. The value of by-product hydrogen has increased with rising oil prices and environmental concerns. Therefore, high-grade use of by-product hydrogen is required in petrochemical complexes. Some researchers suggested a hydrogen recycling network. These case studies demonstrated one of the uses for high-grade by-product hydrogen.[32-33]

Many researches have been conducted to suggest and develop fuel cell power plants for the last decade.[10, 34-37] The feasibility studies have focused on fuel cell power plant systems. Nelson et al. developed a program based on MATLAB to calculate the economic viability PEMFC and SOFC.[38] Lokurlu et al. compared the economics of Combined generation of heat and power (CHP) plants with the economics of fuel cells.[39] Lipman et al. assessed the economic feasibility of a PEMFC power generator using natural gas under various scenarios.[40]

However, a novel fuel cell system, which uses by-product hydrogen, has not been assessed economically. Some studies focused on the introduction of a power

* The partial part of this chapter is taken from the author's published paper in journal.[31]

generation system using by-product hydrogen. PEMFC power plants were installed in Europe. They were connected to a chloro-alkali process, which produced high purity hydrogen.[41] However, the economic and environmental feasibility of these systems have rarely been demonstrated. Therefore, an economic feasibility study on a fuel sell system using by-product hydrogen is necessary for practical application to power generation.

An economic profitability study on a fuel cell power plant that uses by-product hydrogen is presented in this chapter. Some cases were suggested that considered support systems with regular hydrogen purity and variations in prices. Economic assessments were demonstrated for each case. In a technical scenario, development of fuel cell technology was considered based on the prospect of technical progress. The abolition of feed-in tariff and carbon emission trading were considered in a political scenario. Sensitivity analysis was conducted considering carbon credit trends in the discussion chapter.

2.2. Process modeling and assumptions

Most of the PEMFC systems usually use hydrogen as a fuel and the development stage has reached a pilot plant that uses by-product hydrogen. The Pressure swing adsorption (PSA) method is used for hydrogen recovery from refinery off-gases. Therefore, PEMFC power plant fueled by-product hydrogen with a PSA unit was economically assessed in this chapter.

PEMFC system is modeled to make up technical scenarios with respect to development of PEMFC technology, i.e. increase of fuel-to-electricity efficiency. In the previous studies, system sizing specifications, stack lifetime, system efficiency and fuel preprocessing units were considered as key factors for economic assessment with process model. In order to consider stationary application, hydrogen recirculation and heat recovery system, i.e. CHP, were integrated to fuel cell system for increasing overall efficiency.[10, 37, 42] The performance of process model is summarized in Table 2-1. The electrical and fuel utilization efficiency are estimated for the PEMFC power plant using lumped steady-state model.[43] Figure 2-1 shows the PEMFC systems with hydrogen recycle. In the system model, the rate of hydrogen recirculation is calculated to estimate fuel utilization efficiency. In order to develop a recirculation process for the PEMFC system, an adequate balance system model was required. For this reason, a simple system model was developed.[44-45] The system model is developed by the following equations.

$$i = \frac{j \times A_{cell}}{i_{conv}} \tag{2-1}$$

$$v_{in,H_2,a} = \frac{R \times T_{air}}{P_{atm}} \left(\frac{i}{n(H_2)F} \right) \times Stoic_a \tag{2-2}$$

$$v_{in,air,c} = \frac{R \times T_{air}}{P_{atm}} \left(\frac{i}{n(O_2)F} \right) \times Stoic_c \times Stoic_{air,O_2} \tag{2-3}$$

$$\dot{m}_{in,vapor,a} = \frac{P_{atm} \times M_w(H_2O) \times v_{in,vapor,a}}{R \times (T_{in,a} + 273.15)} \tag{2-4}$$

$$\dot{m}_{in,vapor,c} = \frac{P_{atm} \times M_w(H_2O) \times v_{in,vapor,c}}{R \times (T_{in,c} + 273.15)} \tag{2-5}$$

$$v_{vapor,cell} = \frac{R \times T_{cell}}{\left(P_{atm} + \frac{P_{vapor,c}}{P_{k,Pa}} \right)} \times \left(\frac{i}{n(H_2)F} \right) \tag{2-6}$$

where $Stoic_a$ and $Stoic_c$ are constants depending on simulation conditions. Parameters of process modeling are summarized in Table 2-2.

However, PSA unit is not considered. It is assumed that recovery hydrogen has high enough purity for PEMFC system through the PSA unit. The amount of fuel consumption is a major factor in the operation cost which is evaluated by the following equation.

$$F_{in,fuel\_cell} = \frac{P_{demand} \times H_{operation}}{LHV_{H_2} \times \rho_{H_2}} \times \eta_{elec} \times \eta_{util} \tag{2-7}$$

where fuel-to-electricity efficiency is assumed 50% for base case and fuel utilization efficiency is evaluated 95% as maximum.

PEMFC usually operates at low temperature under 100℃. Therefore, the PEMFC power plant could not use heat recovery system in the chemical complex. Otherwise, other high temperature fuel cell, i.e. MCFC, SOFC, could adapt heat

recovery systems which increase the overall system efficiency or generate additional income by selling high temperature steam. In the PEMFC power plant, additional energy provided by CHP is suitable for major housing development. In this study, the PEMFC power plant without CHP is assumed when considering the chemical complex environment.

Stack life time is generally assumed between 3-5 years. Otherwise, Balance of plant (BOP) life time is between 15-20 years which is longer than stack. The 15-year assessment period is determined with assumption of five replacements of stack at the present technology status.

Table 2-1. Comparisons of model performance for economic assessment

Major factor		Hawkes et al. (UK)	Aki et al. (Japan)	Kamarudin et al. (Malaysia)	This study
Process model	CHP	✓	✓	✓	-
	H2 recirculation	-	✓	✓	✓
	PSA	-	-	✓	✓
Stack model	Design parameters for size	-	-	✓	−
	Stack efficiency	✓	✓	-	✓
	Degradation rate	✓	-	-	✓

Table 2-2. PEMFC system modeling parameters

Parameter	Symbol	Value	Unit
Atmospheric pressure	P_{atm}	1	atm
Average atmospheric temperature	T_{air}	25	℃
Anode stoichiometric number	$Stoic_a$	1.5	-
Cathode stoichiometric number	$Stoic_c$	2	-
O_2/air ratio	$Stoic_{air.O2}$	0.2	-
Anode humidifier temperature	$T_{in.a}$	65	℃
Cathode humidifier temperature	$T_{in,c}$	65	℃

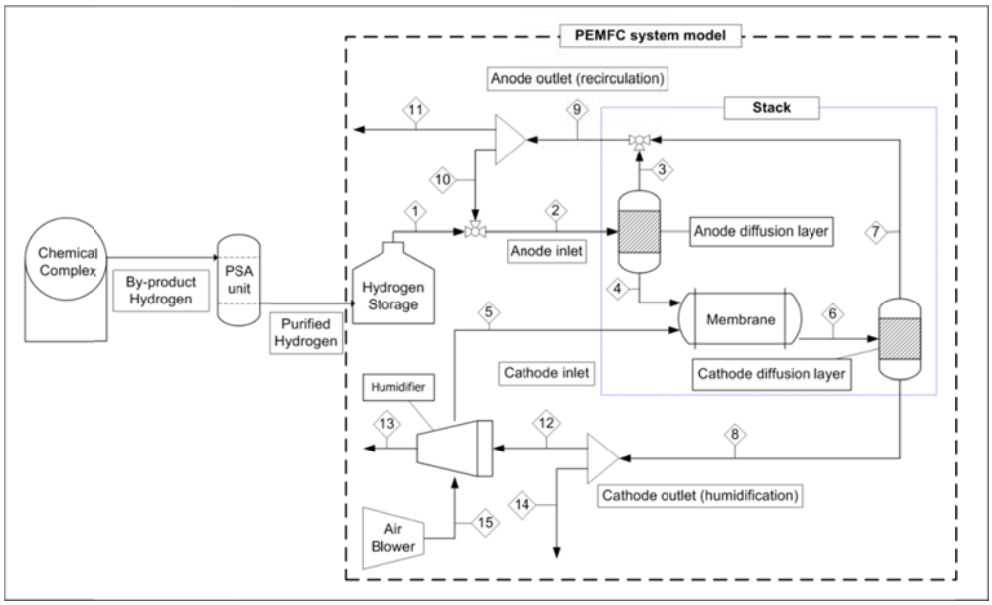

Figure 2-1. Process flow diagram for PEMFC system model.

2.3. Economic assessment

In this chapter, a number of studies describing the cost prediction and technology development have been presented. Economic assessment is evaluated for 15 years with consideration of BOP life time. The parameters for the economic analysis are shown in Table 2-3. Each cost data set with assumptions and corresponding sources are described below.

2.3.1. Capital cost

The total capital cost of a fuel cell power plant was calculated by considering the direct investment cost and indirect investment cost as follows:

$$C_{capital} = C_{direct} + C_{indirect} \tag{2-8}$$

The direct investment cost consisted of the fuel cell system and the PSA system costs. The DOE (Department of Energy, USA) set the cost target values of a PEMFC system in 2011. The target value of the system costs was reduced from \$ 1500/kW to \$ 530/kW at high volume.[46] Therefore, the fuel cell cost, which includes the BOP, was assumed as \$ 1060-3000/kW. The PSA system cost for purification of the by-product hydrogen was also considered in the direct investment cost. A simple model to estimate the cost of the PSA unit was used.[47] The indirect investment cost consisted of the installation cost and introduced the cost of the initial spare parts cost. The direct investment cost and indirect cost were calculated as follows:

$$C_{direct} = C_{fuel\_cell} + C_{PSA} \tag{2-9}$$

$$C_{PSA} = a_{PSA} + b_{PSA} \times F_{in,PSA} \tag{2-10}$$

$$C_{indirect} = C_{install} + C_{introduced} \quad (2\text{-}11)$$

2.3.2. Operation and maintenance cost

In general, Operation and maintenance (O&M) cost included fuel cost, Repair and maintenance (R&M) cost, and fuel cell replacement cost and was calculated as follows:

$$C_{O\&M} = C_{fuel} + C_{maintenance} + C_{replacement} \quad (2\text{-}12)$$

In several studies, the hydrogen production cost was reported as $ 0.99-2.45/kg for conventional steam reforming with the PSA system. For the base case, the hydrogen production cost was assumed as $ 1.25/kg using the average value in the literature.[48-49] The price of by-product hydrogen is also affected by variations in the naphtha price. Therefore, it is assumed that the price of the by-product has a linear relation with the naphtha price, $ 1,116/ton at present, for the case with the highest hydrogen production cost. The equation, which is derived from data in Korea, is as follows.[50]

$$C_{fuel} = C_{byproduct,H_2} \times F_{in,fuel\_cell} \quad (2\text{-}13)$$

$$C_{byproduct,H_2} = 0.01841 \times C_{Naphtha} + 0.49795 \quad (2\text{-}14)$$

The R&M cost is needed when failures in the systems arise for several reasons. Since the stack lifetime is usually shorter than the BOP and the PSA unit lifetime, the maintenance cost, which contains the cost to replace some components except for stack, was determined by the following equation.

$$C_{maintenance} = 0.2 \times C_{direct} \quad (2\text{-}15)$$

The stack has to be replaced every three or five years within the analysis period. The fuel cell replacement cost is the value to replace the stacks, and it was assumed as a specific percentage of the fuel cell system cost when considering the Capital recovery factor (CRF) and was calculated as follows:

$$C_{replacement} = CRF \times C_{fuel\_cell} \times 0.4 \tag{2-16}$$

$$CRF = \frac{i \times (1+i)^{lifetime}}{(1+i)^{lifetime-1}} \tag{2-17}$$

where i is interest rate based on length of one interest period in Table 2-3.

2.3.3. Feed-in tariff

In Korea, the feed-in tariff will be abolished in 2012. However, several governments in Asia and other countries, such as India, Indonesia, Philippines, Thailand, Pakistan, China, USA, Spain, South Africa, Italy, Portugal, and Greece, will hold to the feed-in tariff policy that has proven to be a successful support system in bringing about renewable power plants at low costs.[51-52] Therefore, the policy was also considered to evaluate the effect of the feed-in tariff within carbon emission trading in global competitiveness.

2.3.4. Carbon emission trading

Certified emission reduction (CER), also known as carbon credit, is a permit representing the right to emit carbon dioxide. When power plants generate electricity by renewable energy, CER was created to substitute conventional electricity production and subsequent emissions. Carbon credit that has the effect of increasing income was assumed as \$ 15/ton(CO_2) based on average price in EU

emissions trading system.[53] The amount of emission reduction was calculated equivalent to the amount of carbon dioxide emission for conventional electricity production (0.0004448 ton(CO_2)/kWh).

2.3.5. Income

Most of profit is generated from electricity sales in the PEMFC power plant. The base case assumed that the electricity price was decided by Sales marginal price (SMP) instead of the feed-in tariff. For the case study, we considered a change in income due to not only a hold up of the feed-in tariff but also to adaptions in carbon emission trading. In the discussion chapter, we created a scenario that changed the period the feed-in tariff was maintained to assess the economic feasibility.

2.3.6. Economic feasibility

Cash flow shows the representative monetary flow at each instance in the whole project. The cash flow covered annual cost and income including tax and depreciation charge. The total project cash flow was a combination of net profit after taxes and the depreciation charge. The net profit was justified as the difference between annual income and cost. The cost included the fuel cost, operation and maintenance cost, replacement cost, and depreciation charge. The tax rate was set to 20% from government statements. In order to calculate the annual percentage rate of depreciation for 15 year recovery period asset, the Modified accelerated cost recovery system (MACRS) depreciation rate used. The cash flow was calculated according to the following equation. [54]

$$CF_n = \left(Income_n - C_{O\&M,n} - C_{Depreciation,n} \right) \times \left(1 - Tax \right) + C_{Depreciation,n} \quad (2\text{-}18)$$

where n is year under consideration.

The cash flow for each year was refunded to the initial investment pool as the capital cost. The annual cash flow and the initial investment cost naturally reflected the time value of the money with interest at a rate of 3%. The present value of the money was calculated with the compound interest method.

The profit anticipated from the initial capital costs was evaluated by following profitability standard. Annual Net present value (NPV) was justified as the total present value of the accumulated cash flows minus the present value of the initial investment. The annual NPV of the fuel cell power plant project was justified with the following equation.

$$NPV_n = \left[\sum_{k=1}^{n} (1+i)^{-k} \times CF_k \right] - C_{capital} \tag{2-19}$$

Also, the annual NPV might be calculated for the entire project period. This value called total NPV indicates the economic feasibility of the target project. The total NPV of the fuel cell power plant project was justified with the following equation.

$$NPV_t = \left[\sum_{i=1}^{15} (1+i)^{-k} \times CF_k \right] - C_{capital} \tag{2-20}$$

The economic feasibility of the fuel cell power plant project is positively demonstrated when the result of the total NPV at the end of the project year is a positive value. Furthermore, the project reaches the break-even point when the annual NPV exceeds a zero value. Therefore, the project was demonstrated and compared with various technical and political scenarios. Calculations based on the proposed equations with the cash flow was programmed using an excel flowsheet that was coded with Visual Basic.

Table 2-3. Technical data and base data for economic assessment

Section	Parameter name	Symbol	Value	Unit	Data source
System data	Power demand	P_{demand}	1071	kW	Manufacturer
	H_2 density	ρ_{H2}	0.08988	kg/m^3	Reference [55]
	Low heating value of H_2	LHV_{H2}	120.1	MJ/kg	Reference [55]
	Efficiency of electric	η_{elec}	0.5	dimension less	Reference [46]
	Efficiency of fuel utilization	η_{util}	0.95	dimension less	Estimated
	Operation hour	$H_{operation}$	7884	hrs	Manufacturer
	Degradation rate of power		12	%	Manufacturer
Capital cost	Total cost of fuel cell	C_{fuel_cell}	3,213,000	$	Estimated
	Total cost of PSA	C_{PSA}	327,945	$	Estimated
	Cost of fuel cell	$C_{install}$	1,062,286	$	Estimated

	installation				
	Cost of system introduced	$C_{introduce}$	991.467	$	Estimated
	Fitting constant	a_{PSA}	503.8	dimension less	Reference [33, 47]
	Fitting constant	b_{PSA}	347.4	dimension less	Reference [33, 47]
	Flow rate demand for PSA	$F_{in,PSA}$	942.57	Mscfd	Estimated
O&M cost	Cost of by-product H_2	$C_{byproduct,H2}$	1.25	$/kg	Reference [48-49]
	Cost of naphtha	$C_{Naphtha}$	133.01	$/barrel	Market
	Amount of H_2 demand for fuel cell	$F_{in,fuel\_cell}$	518,492	kg/yr	Estimated
	Fuel cell life time	*lifetime*	3	yrs	Manufacturer
Income	Cost of electricity	COE	153.13	Won* /kWh	Market
	Certified	CER	0.000444	ton(CO_2)/	Market

	emission reduction		8	kWh	
	Carbon credit	C_{CER}	10	\$ /ton(CO_2)	Reference [56]
Cash flow	Interest rate	*i*	0.03	dimension less	Market
	corporate tax rate	*Tax*	0.20	dimension less	Market
	Escalation rate of COE		0.02	dimension less	Market
	Escalation rate of fuel cost		0.02	dimension less	Market

2.4. Case study

Process model provides the amount of fuel consumption and power generation for case study. Degradation of stack catalyst and stack efficiency are calculated based on specification, i.e. system efficiency, that is assumed in the technical scenario. Structure of economic analysis shown in Figure 2-2.

2.4.1. Technical scenario

The DOE target for a stack lifetime was expanded from 20,000 to 40,000 hours and the efficiency with reformer was increased from 32% to 40%. In a study on a small stationary fuel cell, the estimated High heating value (HHV) efficiency was reported as 53.1-82.1% taking into consideration the system efficiency.[46, 57] Therefore, the stack lifetime and efficiency for our case study were modified to 3-5yrs and 49.8-60%, respectively. The fuel cell cost, which was a fixed investment the first year, and the change in replacement cost due to technical development in extending the stack lifetime are the most important factors in determining the overall cost. To evaluate the cost effect of technical development, we assumed three cases that consisted of high cost for base case and medium and high cost cases that decreased the system cost and increased the efficiency through the extension of the stack lifetime shown in Table 2-4. Process model estimates the fuel consumption rate and the power output with considering the system efficiency and the stack life time.

2.4.2. Political scenario

The feed-in tariff is one of the policies that address the incentive to investment for renewable energy. Many developed countries and developing countries are

maintaining the feed-in tariff for eco-friendly power generation systems, such as fuel cells, wind, solar, etc. Therefore, the political scenario consisted of four cases that considered whether a feed-in tariff was suggested. For carbon emission trading, a scenario was assumed in the same manner as shown in Table 2- 5.

2.4.3. Estimation of NPV

With regard to both of the technical and the political scenarios used in the case study, NPV was calculated with a fuel cost of $ 1.25/ton(H_2) shown in Figure 2-3. All NPVs of the high system cost cases used recent data, indicated the deficit, and considered the low cost of byproduct hydrogen. According to the development level of technology, the NPV gradually increased toward a surplus benefit. With the assumption of a support system (case A, case B, case AB) existing, the NPV of low system cost cases show beneficial results. However, the scenario of the medium system cost was dependent on the effect of the support system whether NPV was positive. If cost of naphtha is assumed at present $ 1,116/ton, the by-product hydrogen cost is calculated $ 2.5/ton(H_2) by Equation (2-14). Only two cases had economic benefit with the feed-in tariff and with the assumption of a low system cost shown in Figure 2-4. To verify the effect of the support systems, such as the feed-in tariff and carbon credit, a sensitivity analysis was done in the next chapter.

Table 2-4. Summary of the technical scenarios

Description	High	Medium	Low
System cost ($/kW)	3000	2000	1060
System efficiency (%)	50	55	60
Stack lifetime (yrs)	3	4	5

Table 2-5. Summary of the political scenarios

Description	Base Case	Case A	Case B	Case AB
Electricity cost (Won*/kWh)	153.13**	153.13**	265.84***	265.84***
Carbon price (€/ton(CO_2))	-	10	-	10
Feed-in tariff	No	No	Yes	Yes
CER	No	Yes	No	Yes

* South Korean won

** Average SMP price (2011)

*** Applying the feed-in tariff (2010)

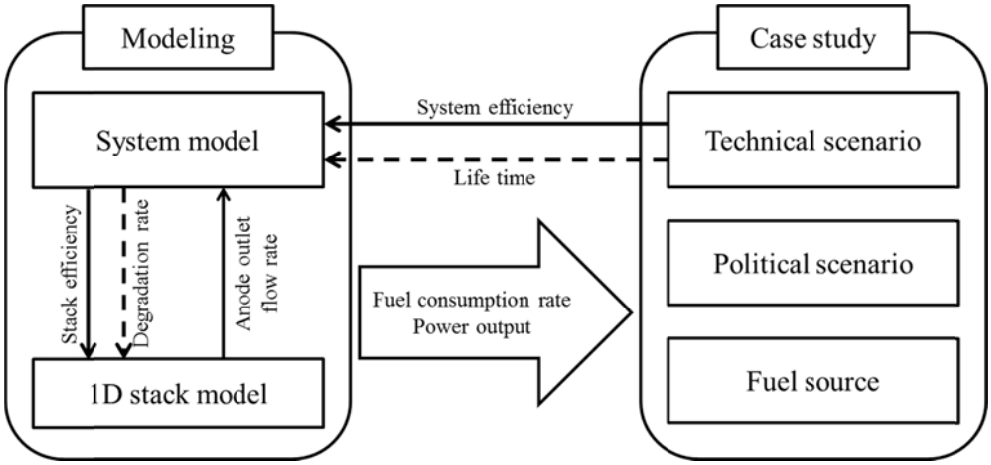

Figure 2-2. Structure of economic analysis with modeling and case study.

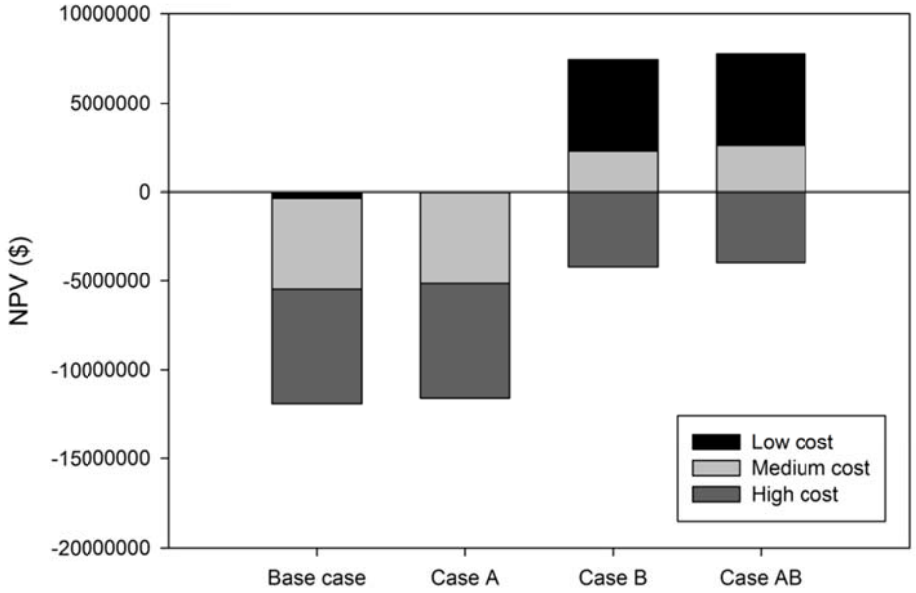

Figure 2-3. Comparison of NPV for a fuel cost of $ 1.25/kg H_2.

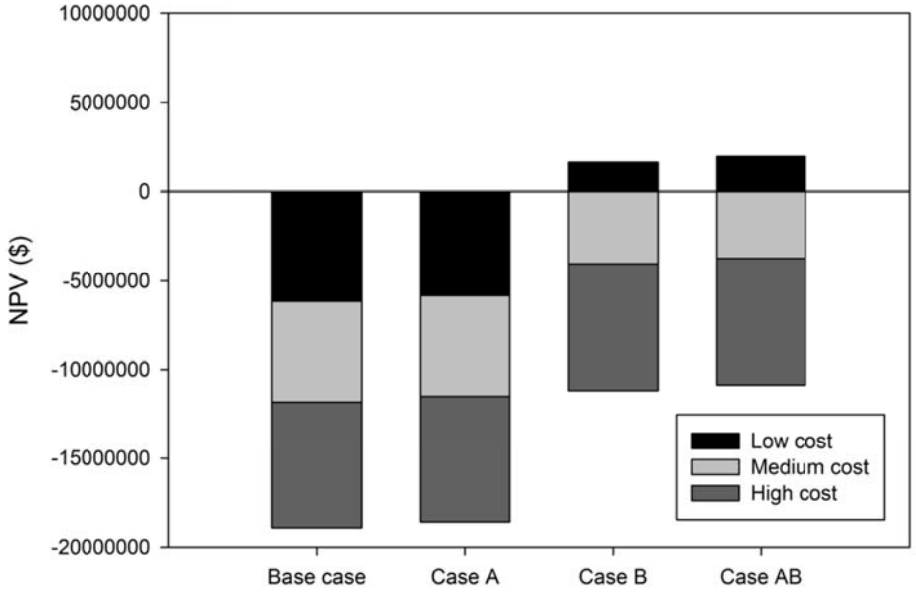

Figure 2-4. Comparison of NPV for a fuel cost of $ 2.50/kg H_2.

2.5. Results and discussion

Several NPV results of case studies have indicated investment in fuel cell power plants using by-product hydrogen as a fuel gas has no economic feasibility at the present stage technical development. However, progress in developing fuel cell technology has been reported annually. The investment of the case AB has an economic feasibility within the low system cost through the technical development.

A support system by the government and the driving force of the global market were prepared. Especially, the feed-in tariff is known as an effective incentive system to expand the deployment of renewable energy systems and it was considered in our sensitivity analysis. Carbon credit is changed by market circumstances, e.g. the trend in the EU carbon dioxide allowance (EUA) price showed great fluctuation between € 5-30/ton(CO_2) from 2003 to 2006.[58] Other research predicted EUA price between 10-€ 100/ton(CO_2) from 2010 to 2030.[56] Therefore, variations in the CER prices were also considered in our study. Figure 2-5 shows the cash flow of case A with a fuel cost of $ 1.25/ton(H_2) and a low system cost in terms of the annual NPV. If the CER price was greater than $ 10/ton(CO_2), the annual NPV was positive at the end of analysis period. Though, without the feed-in tariff, the annual NPV was turned around to positive in less than 10 years for a CER price above $ 40/ton(CO_2). Along with the increasing CER price, the surplus beginning year shortened shown in Figure 2-6.

To evaluate the effect of another support system, a sensitivity analysis was done considering a change in the period the feed-in tariff was maintained. After abolition of the feed-in tariff, a CER price of $ 10/ton(CO_2) was assumed for the remaining period. Since the medium system cost with a fuel cost of $ 1.25/ton(H_2) and the

low system cost with \$ 2.5/ton(H_2) have economic feasibility in the case study, we considered both cases for the sensitivity analysis. Figure 2-7 shows that maintaining the period of the feed-in tariff was essential in ensuring economic benefit when the CER price range varied from \$ 5 to \$ 100 (/ton CO_2). In the analysis, if the CER price was greater than \$ 30 (/ton CO_2) in the near future, the period for maintaining the feed-in tariff was shortened by less than 10 years for both cases. A significant beneficial contribution is made by the feed-in tariff.

As aforementioned, the investment of the PEMFC power plant has an economic feasibility in some cases with variation of CER price and feed-in tariff. These case studies are considered one hydrogen source using by-product hydrogen with PSA unit. However, there are various hydrogen sources that produced by converting fossil fuel to hydrogen or renewable energy to hydrogen, i.e. gasoline, natural gas, wind and solar. Capital cost is decreased because PSA unit is not considered, but average price of hydrogen is increased from \$ 3.00 to \$ 4.00 (/kg H_2) by the energy sources.[59] Both AB case of high and low hydrogen cost using by-product hydrogen have a positive NPV, but others have a negative NPV as shown in Figure 2-8. Therefore, usage of by-product hydrogen has an economic benefit.

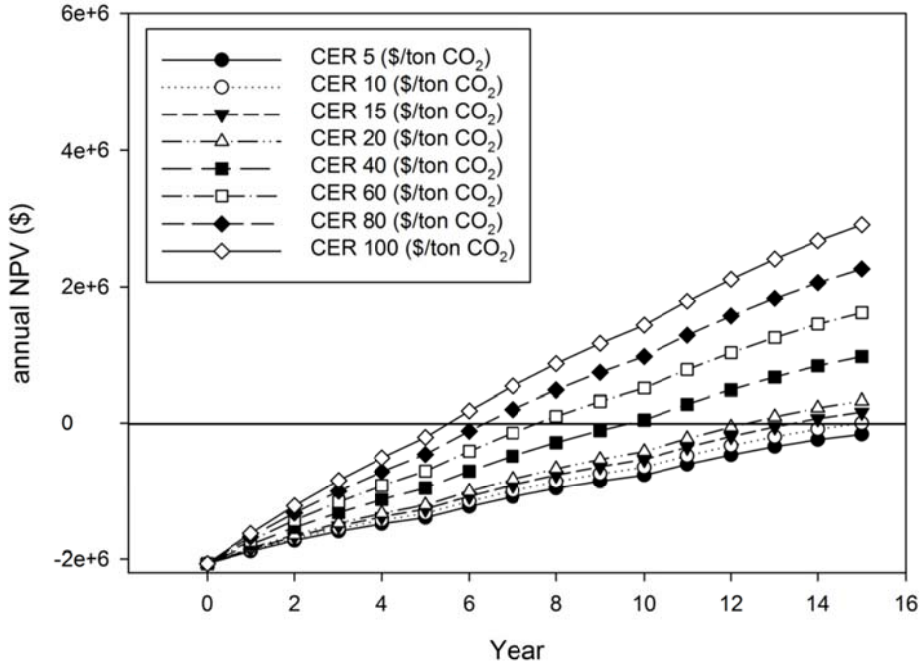

Figure 2-5. Annual NPV with variations in the CER prices (Low cost, fuel price of $ 1.25/kg H_2, no feed-in tariff).

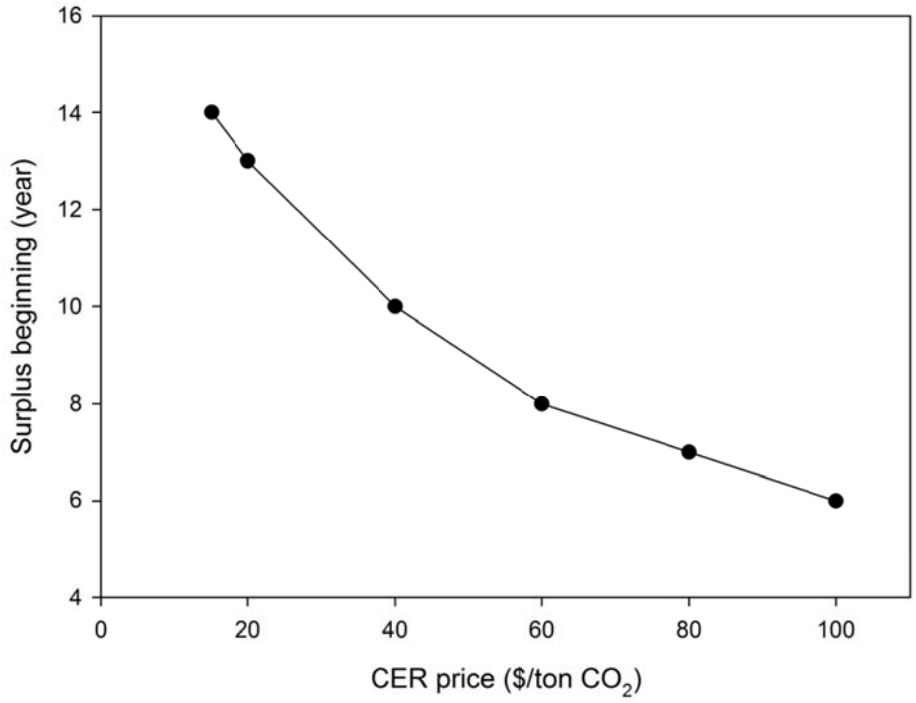

Figure 2-6. Estimated surplus beginning year in cash flow with variations in the CER prices (Low cost, fuel price of $ 1.25/kg H_2, no feed-in tariff).

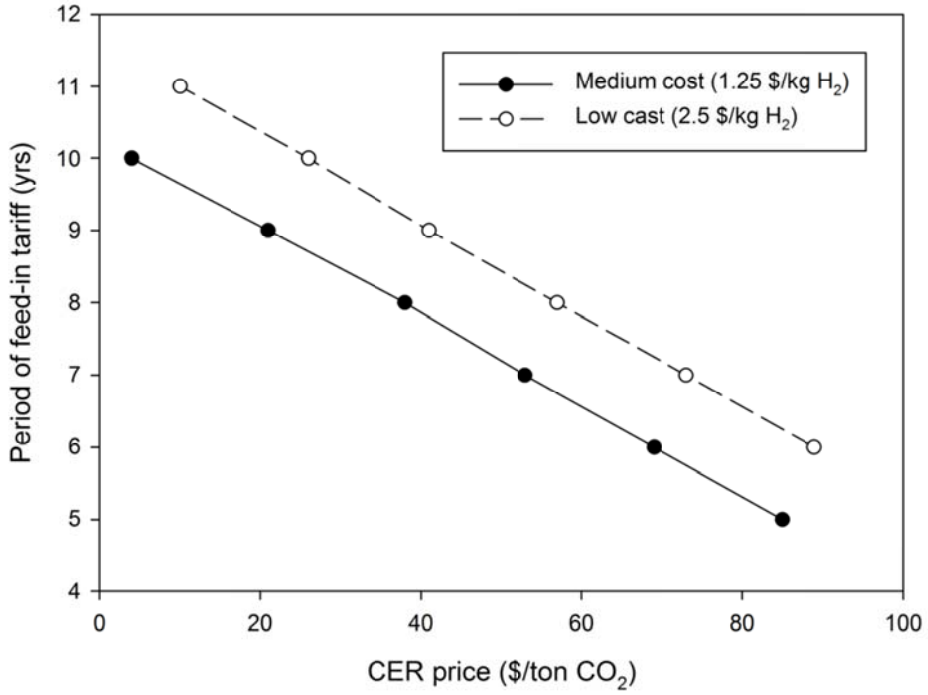

Figure 2-7. Sensitivity analysis of the feed-in tariff period with variations in the CER prices.

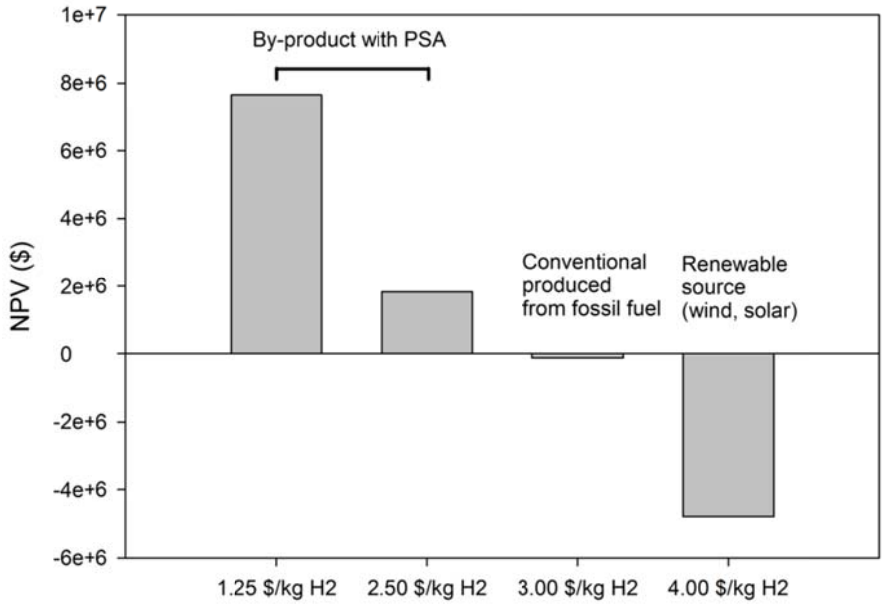

Figure 2-8. Comparison of NPV for AB case with variations in the hydrogen sources (Low cost).

2.6. Conclusions

The economic feasibility of a fuel cell power plant using by-product hydrogen as a fuel gas was assessed under various assumptions. By-product hydrogen has some advantages such as a fuel for fuel cells due to its low price and environmental aspects. However, a PSA system is necessary to purify the by-product hydrogen from the off-gas. This chapter assessed fuel cell economics taking into consideration the level of technical development, fuel cost, support systems, and CER prices. Study cases were developed from the base case. In terms of the technical scenario considering the system cost, the efficiency and system lifetime and the development of fuel cell technology are very important in achieving profitability. Support systems made the economics of the fuel cells more profitable in cases A, B, and AB. We also took into consideration variations in the support systems under a political scenario. The feed-in tariff has more beneficial effects than the CER price. The surplus beginning year was estimated with the annual NPV without the assumption of a feed-in tariff. Under a low system cost scenario, the annual profit will be determined by the CER price.

Feed-in tariffs have a strong effect on the economics of fuel cells using by-product hydrogen. Therefore, maintaining the feed-in tariff is important in expanding the deployment of fuel cell power plants. Development of fuel cell technologies is also a significant factor on the economics of fuel cells. Extensive development of fuel cell technology is needed to make the no feed-in tariff condition profitable. Adequate support systems are also needed to assist in the operation of fuel cells. Fuel cells using by-product hydrogen may have an important role in electric generation when electricity has high price rates.

CHAPTER 3 : Modeling and Simulation of PEMFC for Understanding Transport Phenomena†

3.1. Introduction

Most research focuses on single cells and stacks such as membranes, catalysts, and Gas-diffusion layers (GDLs). Increasingly, the focus has been on the design of a system using PEMFCs.[61-64] Detailed analysis in a fuel cell system is more complex than in a single cell or stack because the rigorous model of a single cell or stack is too complicated for simultaneously solving the problems of a fuel cell system.[65-66] This chapter presents a 2D steady-state mathematical model and a 3-segment dynamic model that can be used for the analysis of water content at the channel outlet and membrane.

Water content has an important role in PEMFCs.[67-69] Occasionally, the water content of the outlet gas purge due to temperature difference is omitted at low electrical load levels. However, the water content at the channel outlet is important for decreasing the volume of the water tank for the hydrogen recirculation system in a fuel cell vehicle.[70] At the first, steady-state model is needed, which is help for understanding of transport phenomena in a single cell. Water content in the membrane is related to the water flooding which is cause of decreasing the amount of gas transportation through the GDL. Otherwise, lack of water vapor in the GDL has negative effect to membrane hydration.[71-74] When the state of membrane is dehydration, the amount of proton transport through membrane decreased. Both of

† The partial part of this chapter is taken from the author's submitted paper in journal.[60]

flooding and dehydration is negative factor for the overall performance of power generation. These two states of membrane are rigorously estimated by using 2D model. On the other hand, improve design specifications, a dynamic model is needed, which can estimate the amount of water near the membrane and the voltage in several regions with considering time variation.[75] In the stack, the amount of water vapor generation is higher than in a single cell. The effect of current variation on the amount of water vapor in the outlet gas flow was quantitatively analyzed to increase the volumetric efficiency and to improve the water management of a fuel cell system with a modified dynamic stack model.

3.2. Voltage modeling and assumptions

In both of steady-state model and dynamic model, voltage model usually consists of Open circuit voltage (OCV) model and three loss factor models. OCV is theoretical maximum voltage based on Gibbs free energy in a cell with following reaction.[76-77]

$$H_2 + \frac{1}{2} O_2 \rightarrow H_2O \tag{3-1}$$

Gibbs free energy of formation is derived by following equation.

$$\begin{aligned} \Delta g_f &= g_f\left(product\right) - g_f\left(reactant\right) \\ &= \Delta g_f^{\mathrm{O}} - RT_{fuelcell} \ln\left[\frac{P_{H_2} P_{O_2}^{1/2}}{P_{H_2O}}\right] \end{aligned} \tag{3-2}$$

$$E = \frac{-\Delta g_f}{2F} = 1.229 + \left(T_{fuelcell} - T_{atm}\right)\left(\frac{\Delta S^{\mathrm{O}}}{2F}\right) \tag{3-3}$$

where T_{atm} = 25℃ and formation of liquid water product $\Delta S^{\mathrm{O}} = 164.0245\, J/K$ with reversible reaction assumption. Equation (3-3) is general form of OCV model. Parameters are modified using nonlinear regression based on experimental performance data.[17] OCV model is can be expressed by following equation.

$$\begin{aligned} E &= 1.229 - 8.5e^{-4}\left(T_{fuelcell} - 298.15\right) \\ &+ 4.308e^{-5} T_{fuelcell}\left[\ln\frac{P_{H_2}}{1.01325} + \frac{1}{2}\ln\frac{P_{O_2}}{1.01325}\right] \end{aligned} \tag{3-4}$$

Activation loss, ohmic loss and concentration loss are important loss factors decreasing overall voltage. Activation loss model is modified Tafel equation for

estimation of cathode loss dominant with following equation.[78]

$$v_{act} = v_0 + v_a \left(1 - e^{-c_1 i}\right) \tag{3-5}$$

where v_0 is voltage drop at zero current density and c_1= 10 . Parameters are determined by experiment data with following equations.[76, 79]

$$\begin{aligned} v_0 &= 0.279 - \left(T_{fuelcell} - 298.15\right) \\ &+4.308e^{-5} T_{fuelcell} \left[\ln\left(\frac{P_{ca} - P_{sat}}{1.01325}\right) + \frac{1}{2}\ln\left(\frac{P_{ca} - P_{sat}}{1.01325}\right)\right] \end{aligned} \tag{3-6}$$

$$\begin{aligned} v_a &= \left(-1.618e^{-5} T_{fuelcell} + 1.618e^{-2}\right)\left(\frac{P_{O_2}}{0.1173} + P_{sat}\right)^2 \\ &+\left(1.8e^{-4} T_{fuelcell} - 0.166\right)\left(\frac{P_{O_2}}{0.1173} + P_{sat}\right) \\ &+\left(-5.8e^{-4} T_{fuelcell} + 0.5736\right) \end{aligned} \tag{3-7}$$

where P_{ca} is cathode pressure and P_{sat} is saturation pressure.

Ohmic loss model can be derived by following Ohm's law.[79]

$$v_{ohm} = iR_{ohm} \tag{3-8}$$

$$R_{ohm} = \frac{t_m}{\sigma_m} \tag{3-9}$$

where t_m is thickness of membrane and σ_m is membrane conductivity.

When operation condition is low current density, concentration loss is infinitesimal amount of overpotential. However, at high current density, consumption rate of reactant is increased. Especially, oxygen concentration difference between catalyst layer and channel is critical source of concentration overpotential in the cathode side. Concentration loss is usually determined

empirically. In this voltage model, Guzzella's concentration model is adopted with following equations.[80]

$$v_{conc} = i\left(c_2 \frac{i}{i_{\max}} \right)^{c_3} \tag{3-10}$$

where i_{max} = 2.2 A, c_3 = 2 and c_2 is described by following equation for each condition of pressure.

$$\begin{aligned} c_2 &= \left(7.16e^{-4}T_{fuelcell} - 0.622\right)\left(\frac{P_{O_2}}{0.1173} + P_{sat}\right) \\ &+ \left(-1.45e^{-3}T_{fuelcell} + 1.68\right) \quad \text{for} \quad \left(\frac{P_{O_2}}{0.1173} + P_{sat}\right) < 2atm \end{aligned} \tag{3-11}$$

$$\begin{aligned} c_2 &= \left(8.66e^{-5}T_{fuelcell} - 0.068\right)\left(\frac{P_{O_2}}{0.1173} + P_{sat}\right) \\ &+ \left(-1.6e^{-4}T_{fuelcell} + 0.54\right) \quad \text{for} \quad \left(\frac{P_{O_2}}{0.1173} + P_{sat}\right) \geq 2atm \end{aligned} \tag{3-12}$$

In order to estimate overall voltage, voltage model is derived by following equation.

$$v_{total} = E - v_{act} - v_{ohm} - v_{conc} \tag{3-13}$$

These voltage models are used both 2D steady state model and dynamic model with one dimensional assumption through direction of membrane thickness. For stack simulation, terminal stack voltage is calculated by multiplying v_{total} with number of cells of the stack. Pressure distribution and flow characteristic are described differently for each purpose in following chapters.

3.3. Steady-state modeling and simulation

This chapter proposes a two dimensional steady-state rigorous model based on a first principle of electrochemistry and transport phenomena to calculate the water content in outlet gas flow and membrane.

3.3.1. Assumptions and specifications

In order to validate the model, the experiment consisted of the PRIMEA® membrane and a parallel serpentine flow field. For two dimensional simulation, flow field is assumed flat single channel shows in Figure 3-1. A constant flow rate was fixed to max current density. The basic assumptions of the 2D steady-state cell model are (i) perfect gases; (ii) laminar flow and incompressible fluids; (iii) contact electrical losses are neglected; (iv) isothermal state. During the experiment, the cell temperature was maintained at 65℃, and the humidification condition of inlet gases at the anode and cathode were 100% relative humidity (RH).

3.3.2. Rigorous two dimensional model

In the rigorous two dimensional mode, computation domain is consists of seven layers show in Figure 3-2. Both of anode and cathode side have each channel, GDL, catalyst layer. There is membrane layer between anode catalyst layer and anode catalyst layer.

The cell model follows the general governing equations for transport phenomena in PEMFCs[81-82]:

Mass conservation

$$\frac{\partial u}{\partial x}+\frac{\partial v}{\partial y}=0 \qquad (3\text{-}14)$$

Momentum conservation

$$\frac{1}{\varepsilon}\rho\frac{\partial u}{\partial t}+\frac{1}{\varepsilon}\rho\left(u\frac{\partial u}{\partial x}+v\frac{\partial u}{\partial y}\right)=-\varepsilon\frac{\partial p}{\partial x}+\mu\left(\frac{\partial^2 u}{\partial x^2}+\frac{\partial^2 u}{\partial y^2}\right)+S_x \tag{3-15}$$

$$\frac{1}{\varepsilon}\rho\frac{\partial v}{\partial t}+\frac{1}{\varepsilon}\rho\left(u\frac{\partial v}{\partial x}+v\frac{\partial v}{\partial y}\right)=-\varepsilon\frac{\partial p}{\partial y}+\mu\left(\frac{\partial^2 v}{\partial x^2}+\frac{\partial^2 v}{\partial y^2}\right)+S_y \tag{3-16}$$

Species conservation

$$\frac{1}{\varepsilon}\frac{\partial X_k}{\partial t}+\frac{1}{\varepsilon}\left(u\frac{\partial X_k}{\partial x}+v\frac{\partial X_k}{\partial y}\right)=\varepsilon D_k\left(\frac{\partial^2 X_k}{\partial x^2}+\frac{\partial^2 X_k}{\partial y^2}\right)+S_k \tag{3-17}$$

Charge conservation

$$\frac{\partial}{\partial x}\left(\sigma_m\frac{\partial \Phi}{\partial x}\right)+\frac{\partial}{\partial y}\left(\sigma_m\frac{\partial \Phi}{\partial y}\right)+S_\Phi=0 \tag{3-18}$$

where u is velocity of x-direction and v is velocity of y-direction. Source terms of each layer are summarized in Table 3-1. Physical parameters are listed in Table 3-2. A detailed description of the cell model and parameters can be found in B. Sunden et al., P. T. Nguyen et al.[55, 83] Terminal voltage of a single cell is estimated by Equation (3-13).

3.3.3. Solving algorithm

The system model can find a solution without difficulty using only a spreadsheet program. In contrast, an analytical solution of the cell model is complex and nonlinear. Commercial package programs, i.e. Fluent, Comsol multiphysics, gProms, have several limitations for solving proposed rigorous model. Commercial packages provide convenience environment for solving partial diffential equations. However, detailed electrochemical reaction could not adopt in these programs. For

example, commercial software do not provide modified equation format such as equation (3-4) and complex parameter equations such as equations (3-6), (3-7). Therfore, the cell model was numerically solved using Visual C++ code, based on a Finite-volume method (FVM) and the Semi-implicit method for pressure linked equation (SIMPLE) algorithm in Figure 3-3.[84-85]

3.3.4. Analysis of water distribution in a single cell

The experimental data for a single cell can be used for model validation. Figure3-4 compares the measured data with the polarization curve prediction. The calculated polarization curve shows good agreement with the experimental performance curve. Velocity profile in a single cell is presented in Figure 3-5. The results show that velocity distribution is suddenly decreased through the channel due to high friction resistance in the inlet edge region.

Figure 3-6 shows the vapor fraction distribution on the anode side along the gas channel and the GDL for various current densities. The result shows that vapor is well dispersed along the gas channel at a high current density in Figure 3-6 (b) and Figure 3-6 (c). However, distribution of vapor is not uniform at a low current density due to the absence of the water generation reaction in Figure 3-6 (a). The vapor water distribution only affects cathode side. Hydrogen distribution is linearly decreased through the channel with no effect from water vapor fraction.

Table 3-1. Summary of source terms in each domian

Layer	S_x	S_y	S_k	S_Φ
Channel	0	0	0	0
GDL	$-\frac{\mu}{K}\varepsilon^2 u$	$-\frac{\mu}{K}\varepsilon^2 v$	0	0
Catalyst layer	$-\frac{\mu}{K_p}\varepsilon_c{}^2 u + E_\Phi\frac{\partial\Phi}{\partial x}$	$-\frac{\mu}{K_p}\varepsilon_c{}^2 v + E_\Phi\frac{\partial\Phi}{\partial y}$	$\begin{cases} H_2 : -\frac{j_a}{2Fc_{total}} \\ O_2 : \frac{j_c}{2Fc_{total}} \\ H_2O : -\frac{j_a}{4Fc_{total}} \end{cases}$	$\begin{cases} anode : j_a \\ cathode : j_c \end{cases}$
Membrane	$-\frac{\mu}{K_p}\varepsilon_m{}^2 u + E_\Phi\frac{\partial\Phi}{\partial x}$	$-\frac{\mu}{K_p}\varepsilon_m{}^2 v + E_\Phi\frac{\partial\Phi}{\partial y}$	0	0

Table 3-2. Physical parameters of steady-state model

Parameter	Symbol	Value	Unit
Air pressure	P_c	2	atm
Fuel pressure	P_a	1	atm
RH of cathode	Φ_c	100	%
RH of anode	Φ_a	100	%
O_2 diffusivity	D_{O_2}	1.0e-5	cm^2/s
H_2 diffusivity	D_{H_2}	2.63e-2	cm^2/s
Vapor H_2O diffusivity	D_{H_2O}	6.0e-2	cm^2/s
Fuel cell temperater	$T_{fuelcell}$	65	℃
Viscosity	μ	1.0e-4	g/cm•s
Porosity in GDL	ε_L	0.4	-
Porosity in Catalyst layer	ε_c	0.28	-

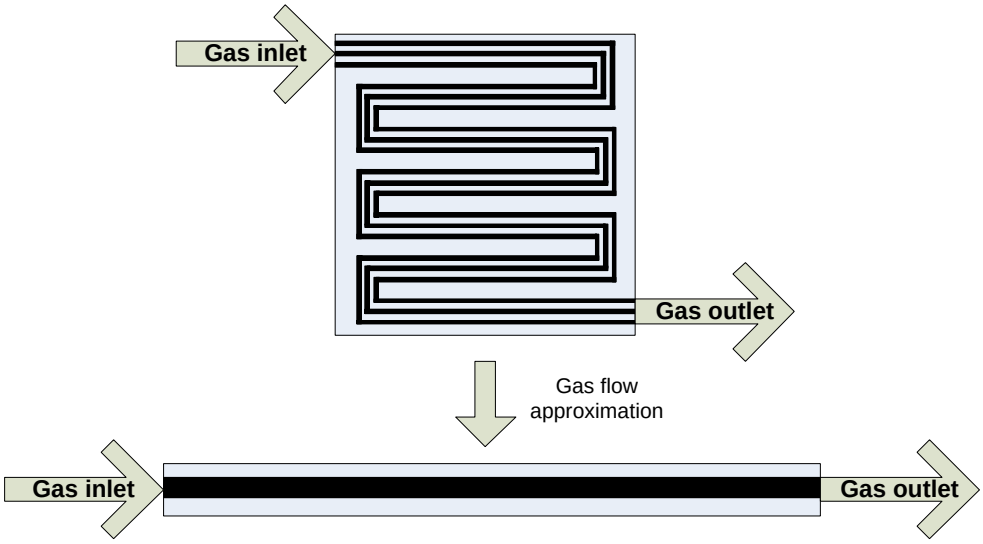

Figure 3-1. Schematic diagram for approximation of gas flow field.

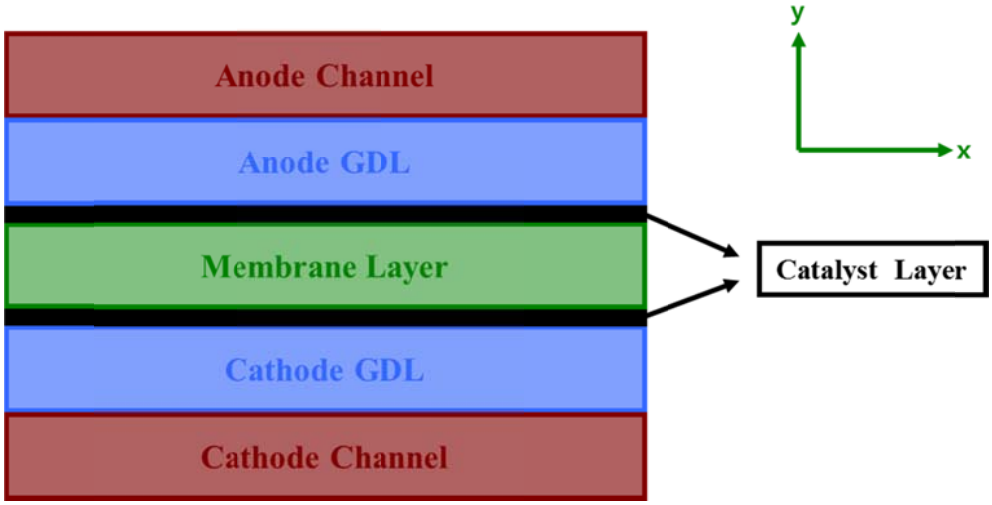

Figure 3-2. Computational domain of two dimensional steady-state model.

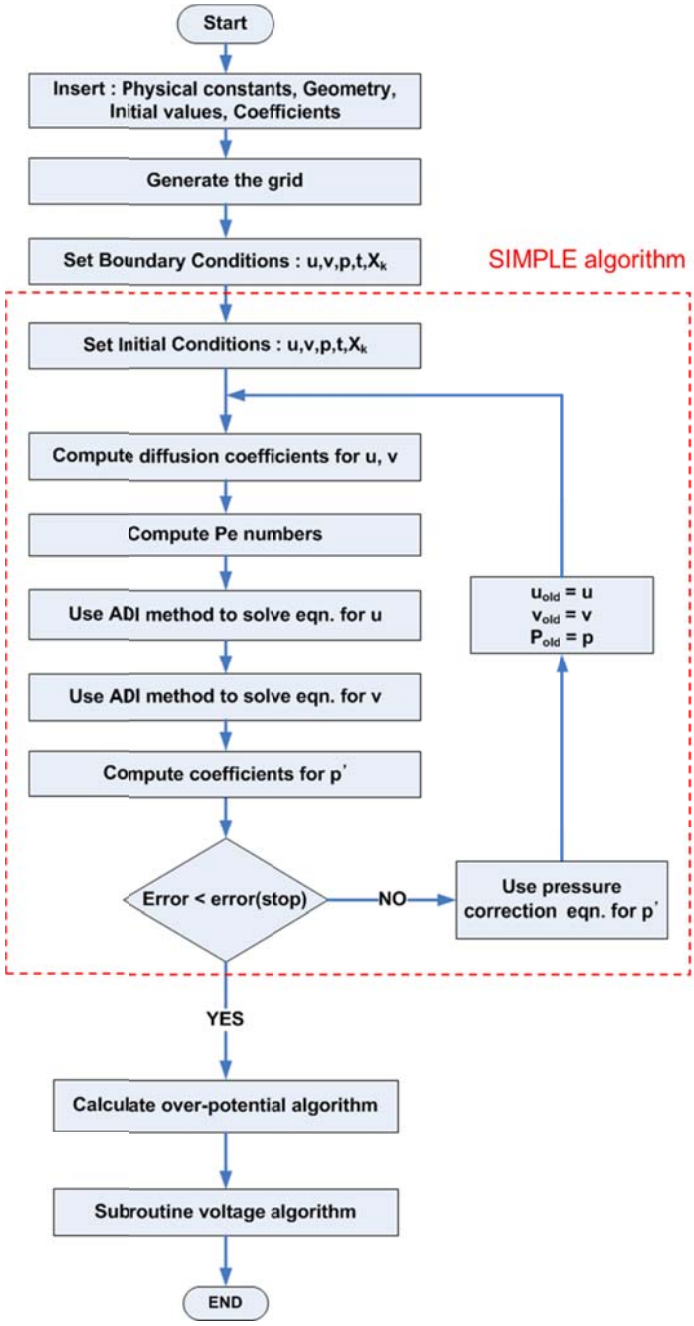

Figure 3-3. Algorithm to estimate solution of two dimensional steady-state model.

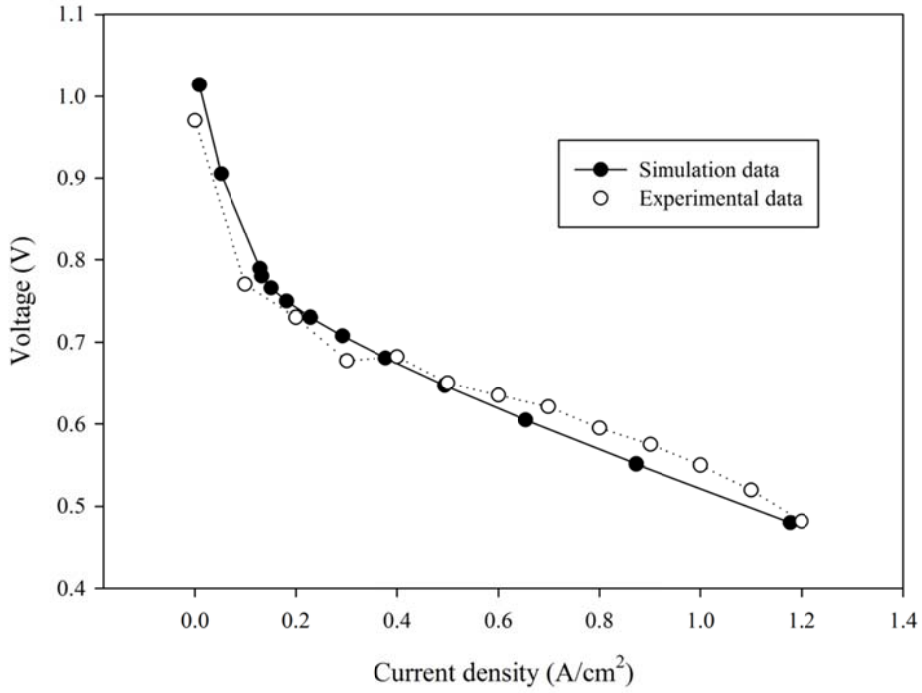

Figure 3-4. Simulation and experimental performance curves for the test cell.

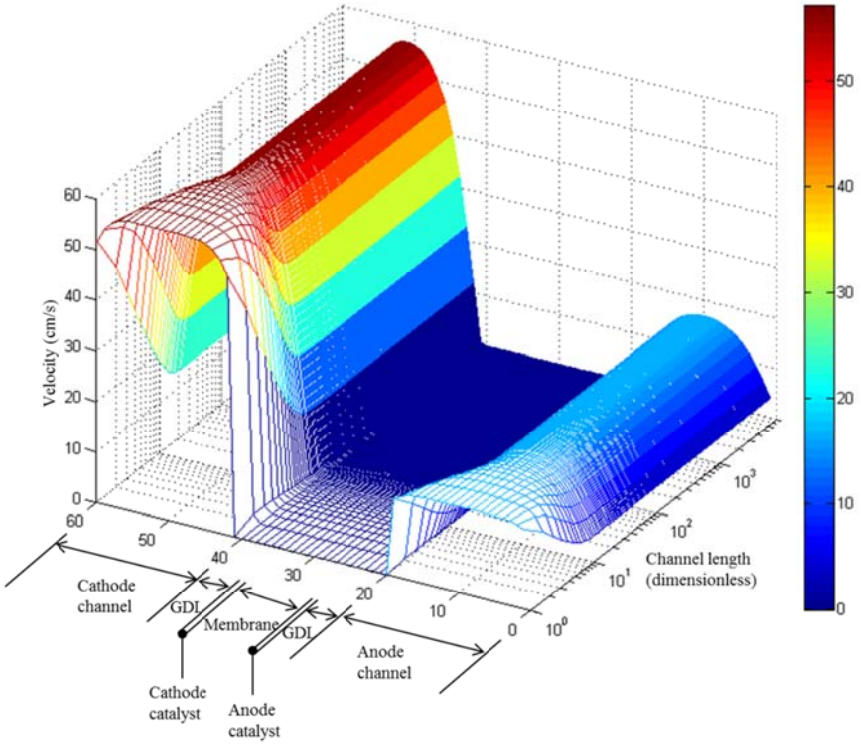

Figure 3-5. Estimation of velocity profile in the single cell for V_{cell} = 0.905 V and I_{avg} = 0.0.052 A/cm^2.

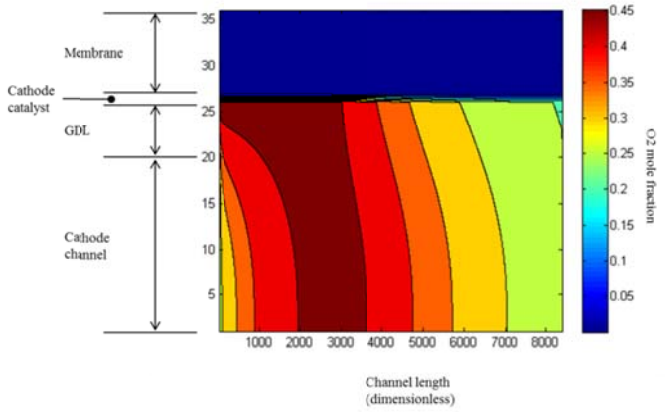

(a)

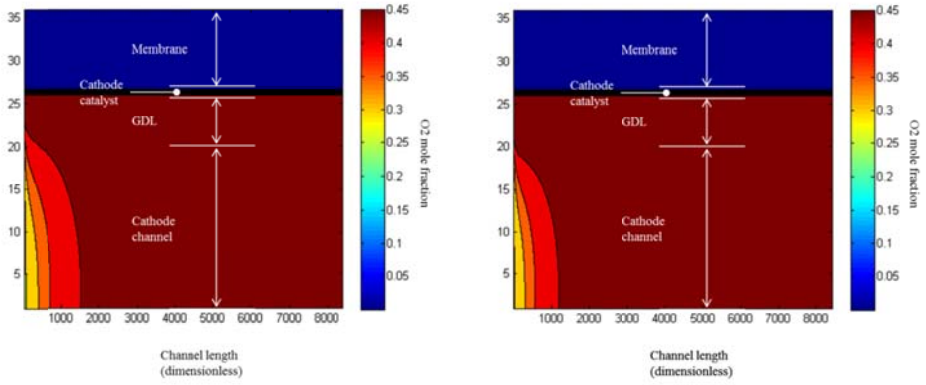

(b) (c)

Figure 3-6. Distribution of vapor mole fraction in the cathode side for (a)V_{cell} = 0.905 V and I_{avg} = 0.0520 A/cm^2, (b)V_{cell} = 0.789 V and I_{avg} = 0.133 A/cm^2, (c)V_{cell} = 0.480 V and I_{avg} = 1.177 A/cm^2.

3.4. Dynamic modeling and simulation

The effect of the amount of current generation on water content in several regions with considering time variation was quantitatively analyzed to increase the volumetric efficiency and improve the water management of a fuel cell system with a modified dynamic PEMFC stack model. This chapter presents a three-segment dynamic stack model for a PEMFC system that can be used to analyze the water content at the channel outlet and membrane.

3.4.1. 3-segment dynamic model

The 3-segment dynamic model is based on the lumped dynamic model. The stack voltage model calculates the terminal stack voltage using equation (3-13) in the lumped dynamic model. The voltage variation of the fuel cell is calculated with an empirically statistic model since the dynamics of the electrochemical reaction are faster than other phenomena such as gas flow and proton transfer. This voltage depends on the current density in the set-point, the partial pressures of hydrogen and oxygen, and the stack temperature. Zero-dimensional dynamic model is consists of cathode flow model, anode flow model and membrane hydration model including the stack voltage model.[86] Scheme of the lumped dynamic model is shown in Figure 3-7.

The cathode flow model provides the dynamics of the cathode outlet gas composition in the cathode channel using variables that include mass conservation, thermodynamic, and psychrometric properties. The dynamics of the cathode outlet gas composition was calculated simultaneously using three other models. The cathode model follows mass balance equations.

$$\frac{dm_{O_2,ca}}{dt} = w_{O_2,ca,in} - w_{O_2,ca,out} - w_{O_2,reacted} \tag{3-19}$$

$$\frac{dm_{N_2,ca}}{dt} = w_{N_2,ca,in} - w_{N_2,ca,out} \tag{3-20}$$

$$\frac{dm_{v,ca}}{dt} = w_{v,ca,in} - w_{v,ca,out} - w_{v,ca,gen} + w_{v,mem} \tag{3-21}$$

Mass flow rates of cathode outlet are calculated by following equations.

$$w_{O_2,ca,out} = x_{O_2,ca} \times w_{air,ca,out} \tag{3-22}$$

$$w_{N_2,ca,out} = \left(1 - x_{O_2,ca}\right) \times w_{air,ca,out} \tag{3-23}$$

$$w_{v,ca,out} = w_{ca,out} - w_{air,ca,out} \tag{3-24}$$

$$x_{O_2,ca} = \frac{y_{O_2,ca} \times M_{O_2}}{y_{O_2,ca} \times M_{O_2} + \left(1 - y_{O_2,ca}\right) \times M_{N_2}} \tag{3-25}$$

where $y_{O_2,ca}$ is oxygen mole fraction in the cathode side. It depends on rate of electrochemical reaction.

The amount of generation in the cathode side is calculated by following equations.

$$w_{O_2,reacted} = M_{O_2} \times \frac{n \cdot i}{4F} \tag{3-26}$$

$$w_{v,ca,gen} = M_v \times \frac{n \cdot i}{2F} \tag{3-27}$$

where *i* is current and *n* is number of cells in the stack.

The anode mass flow model calculates the amount of water vapor and liquid phase across the membrane using water transport information. The anode model follows mass balance equations.

$$\frac{dm_{H_2,an}}{dt} = w_{H_2,an,in} - w_{H_2,an,out} - w_{H_2,reacted} \tag{3-28}$$

$$\frac{dm_{v,an}}{dt} = w_{v,an,in} - w_{v,an,out} - w_{v,mem} - w_{l,an,out}$$

(3-29)

Mass flow rates of anode outlet are calculated by following equations.

$$w_{H_2,an,out} = \frac{1}{1 + \frac{M_v}{M_{H_2}} \cdot \frac{P_{v,an}}{P_{H_2,an}}} \times w_{an,out} \tag{3-30}$$

$$w_{v,an,out} = w_{an,out} - w_{H_2,an,out} \tag{3-31}$$

where $P_{v,an}$ is partial pressure of vapor and $P_{H_2,an}$ is partial pressure of hydrogen in the anode side.

Deprotonating of hydrogen is only one reaction in the anode catalyst layer. Therefore, the amount of hydrogen consumption in the anode side is calculated by following equation.

$$w_{H_2,reacted} = M_{H_2} \times \frac{n \cdot i}{2F} \tag{3-32}$$

The membrane hydration model estimates water transport at the membrane. Electro osmotic drag and back diffusion are driving force of water transport between anode side and cathode side through membrane. Electro osmotic drag is described by following equations.

$$N_{v,osmotic} = n_d \frac{i}{F} \tag{3-33}$$

$$n_d = 0.0029\lambda_m^2 + 0.05\lambda_m - 1.4e^{-14} \tag{3-34}$$

where n_d is electro osmotic drag coefficient and λ_m is membrane water content that depends on the water activity.

Back diffusion is described by following equations.

$$N_{v,diff} = D_w \frac{\left(c_{v,ca} - c_{v,an}\right)}{t_m} \tag{3-35}$$

$$D_w = D_\lambda \exp\left(2416\left(\frac{1}{303} - \frac{1}{T_{fuelcell}}\right)\right) \tag{3-36}$$

where D_w is water diffusion coefficient and D_λ is depends on membrane water contents.

Concentration at the membrane surface is calculated by following equations.

$$c_{v,an} = \frac{\rho_{m,dry}}{M_{m,dry}} \times \lambda_{an} \tag{3-37}$$

$$c_{v,ca} = \frac{\rho_{m,dry}}{M_{m,dry}} \times \lambda_{ca} \tag{3-38}$$

where λ_{an} and λ_{ca} are estimated from activity of the gas with following equations.[61]

$$\lambda_i = \begin{cases} 0.043 + 17.81a_i - 39.85a_i^2 + 36a_i^3 & ,0 < a_i \le 1 \\ 14 + 1.4\left(a_i - 1\right) & ,1 < a_i \le 3 \end{cases} \tag{3-39}$$

$$a_i = \frac{y_{v,i} \cdot P_i}{P_{sat,i}} = \frac{P_{v,i}}{P_{sat,i}} \tag{3-40}$$

The amount of water transports through membrane is calculated by following equation.

$$w_{v,mem} = N_{v,mem} \times M_v \times A_{fuelcell} \times n \quad (3\text{-}41)$$

where $A_{fuelcell}$ is surface area of a single cell.

All input and output variables are summarized in Table 3-3, respectively. Detailed lumped model equations are described in reference.[55, 87]

The lumped dynamic model has been modified to give a more accurate account of the correlation between performance and water distribution. The modified model includes three segments of the entrance region, central region, and exit region. The majority of the stacks were designed for counter-current flow in the gas flow field. The number of segments is determined by this flow field characteristic. The Schematic diagram of flow field and description of segment domain is shown in Figure 3-8. The lumped model has several loops that are computed at the same time via all of submodels. The mass flow rate of the cathode outlet is calculated by the returned manifold pressure and cathode pressure in the lumped model, yet there are no manifolds in the first or second segments. This model assumes that the test station situation has a choke valve, and the calculation loop is simplified for independent simulation of each segment model. Figure 3-9 shows the schematic diagram of calculation loop for the 3-segment dynamic model.

3.4.2. Assumptions and specifications

There are numerous parameters in each submodel. Parameters are determined using nonlinear regression on *i-V* data for the open circuit voltage (OCV) model, the activation loss model, and the concentration loss model. For the ohmic loss model, parameters in the literature were referred to.[88] Assumptions about the model are insignificant anodic activation voltage, uniform current density, and constant

temperature.

Assumptions made for cathode model are ideal gas, variables of exiting flow (T, P, Φ, y) (same as the variables inside the cathode flow channel), and vapor condensation at R.H.≥100%. Spatial variations in each segment are ignored to assume into one volume. Anode model holds the same assumptions as the cathode flow model except for a high-pressure hydrogen storage tank. The assumption specific to the membrane hydration model is that water distribution is uniform throughout the surface area of the membrane.

The operating temperature of the cell was 338.15 K. The physical stack parameters such as the number of cells, surface area of each cell, and total volume of each channel were obtained from the literature to validate the 3-segment model. [87] The stack parameters are summarized in Table 3-4. The simulation condition was 40 % relative humidity on both sides as shown in Table 3-5. Variation of the current for the simulation was set as show in Figure 3-10.

3.4.3. Analysis of water transport through membrane in the stack

The data from the lumped dynamic model can be used to validate the three-segment dynamic model. Figure 3-11 compares the amount of water transport across the membrane of the lumped dynamic model with that of the data from the three-segment dynamic model. The polarization trend curve of water flow agreed with the data from each segment, and the average error was less than 4%. The amount of water transport across the membrane decreased linearly through the channel. The terminal stack voltage is shown in Figure 3-12. The total voltage of

the three-segment model was slightly larger than the terminal voltage of the lumped model. To clarify how the amount of water flow affected the terminal stack voltage, we focused on the water content, representing the degree of hydration, in the membrane. Figure 3-13 shows the water content of the membrane region between the anode and cathode channels from each segment and the lumped model. The water content in segment 1 was larger than the water content in the lumped model since the averaging effect is reflected in the lumped model. The water content of the modified model was dramatically decreased throughout the segment, indicating that the liquid water supply was mainly beneficial for the entrance region of the stack under fuel cell operation. Figure 3-14 shows the element analysis of water transport across the membrane. In the lumped model, the amount of water transferred by osmotic drag was greater than that by back diffusion is shown in Figure 3-14 (a). Osmotic drag decreased as gas flowed to the exit region, which corresponds to the water content of the membrane is shown as Figure 3-14 (b). However, the back diffusion as shown in Figure 3-14 (c) is increased as gas flowed to the exit region, showing a negative effect on the water content. The phenomena of water transport across the membrane slightly affected each segment terminal voltage shown in Figure 3-15. The minimum voltages of segments 1 and 3 were about 79 V and 67 V, respectively. As the gas flows from the entrance segment to the exit segment, the voltage decreased slightly, indicating that the utilization efficiency of the exit segment was smaller than that of the entrance segment. To better understand the effect of water content on the terminal voltage in each segment, we compared voltage elements, such as the OCV, activation loss, Ohmic loss, and concentration loss. The OCV of each segment is shown in Figure

3-15 (b), where the entrance segment has a greater OCV than the exit segment. OCV was calculated with the partial pressures of hydrogen and oxygen. In particular, hydrogen partial pressure had a particularly strong influence on the OCV. Activation and concentration losses increased with the gas flow shown in Figure 3-15 (c) and Figure 3-15 (d). Oxygen partial pressure and saturation pressure were strongly affected by both losses. Figure 3-15 (e) shows the Ohmic loss, which corresponds primarily to the water content of the membrane. This suggests that the development of a performance predictor with the estimation of the water content is required in order to increase the utilization efficiency.

Table 3-3. Input and output variables in the system model

Domain	Category	Variables
Stack voltage model	Input	Stack current
		Cathode pressure
		O_2 Partial pressure
		Stack Temperature
		Membrane water content
		H_2 partial pressure
	Output	Stack Voltage
Cathode flow model	Input	Total mass flow
		Cathode pressure
		O_2 mole fraction
		Membrane water flow
		OM pressure
		Stack voltage
		Stack current
		Stack Temperature
		Relative humidity
	Output	Cathode flow out
		Cathode pressure
		Cathode humidity
		O_2 excess ratio
		Liquid water mass

		O_2 partial pressure
Anode flow model	Input	Total mass flow
		Anode pressure
		Pressure
		Membrane water flow
		Stack voltage
		Stack current
		Stack Temperature
		Relative humidity
	Output	Anode flow out
		Anode pressure
		Anode humidity
		H_2 excess ratio
		Liquid water mass
		H_2 partial pressure
Membrane hydration model	Input	Total mass flow
		Anode pressure
		Pressure
		Membrane water flow
		Stack voltage
		Stack current
		Stack Temperature

	Relative humidity
Output	Anode flow out
	Anode pressure
	Anode humidity
	H_2 excess ratio
	Liquid water mass
	H_2 partial pressure

Table 3-4. Physical stack parameters

Parameters	Value	Unit
Anode total volume	0.005	m^3
Cathode total volume	0.01	m^3
Membrane dry density	0.002	kg/m^3
Membrane dry equivalent weight	1.1	kg/mol
Membrane thickness	1.275e-2	cm

Table 3-5. Simulation conditions

Parameters	Value
Number of cells	381
Unit area	250 cm^2
Temperature	65℃
Relative humidity (R.H.)	anode 40% cathode 40%

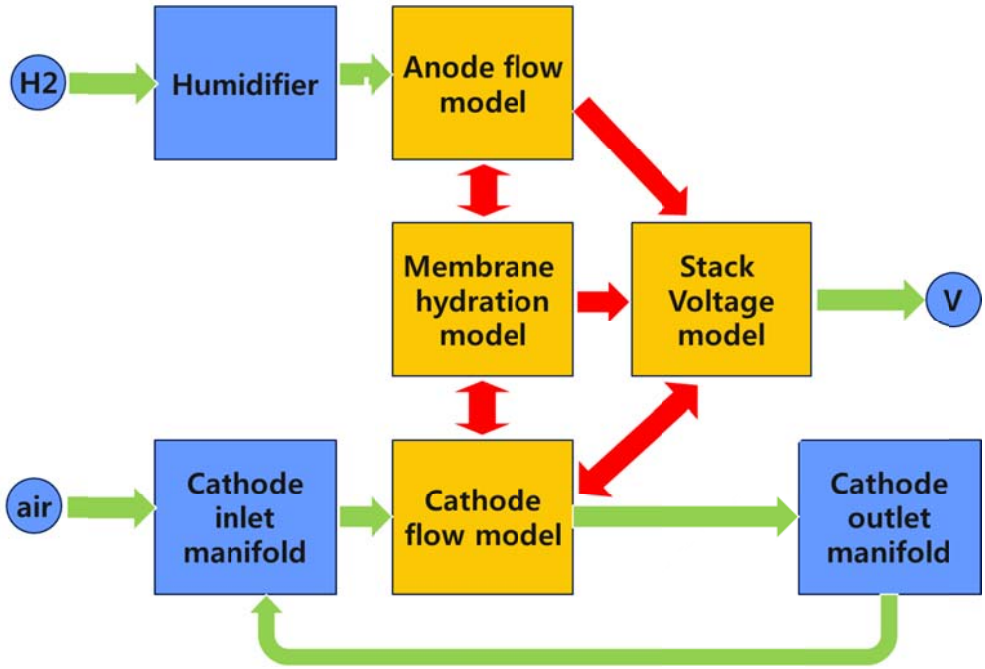

Figure 3-7. Scheme of zero-dimensional dynamic model of PEMFC.

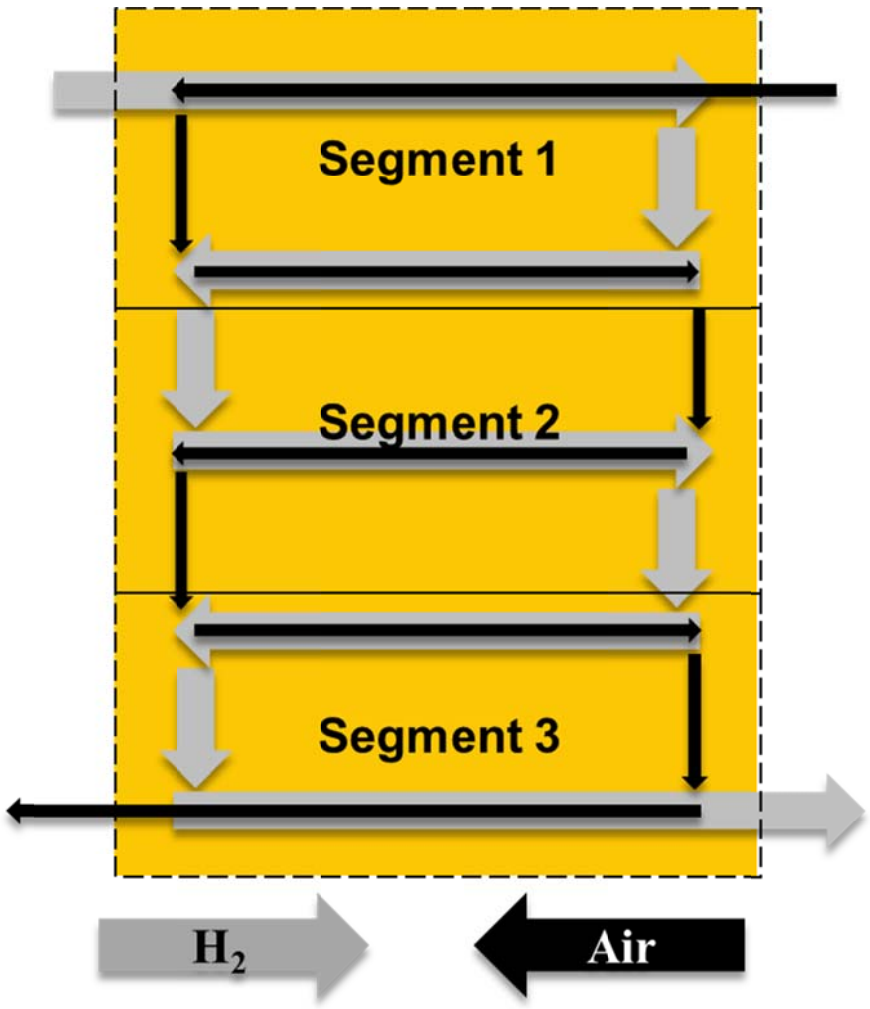

Figure 3-8. Schematic diagram of flow field and description of segment domain.

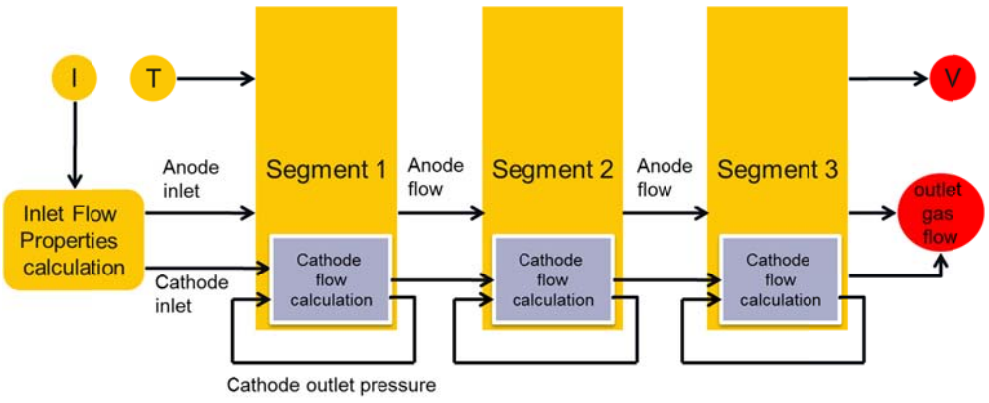

Figure 3-9. Schematic diagram of the 3-segment dynamic model.

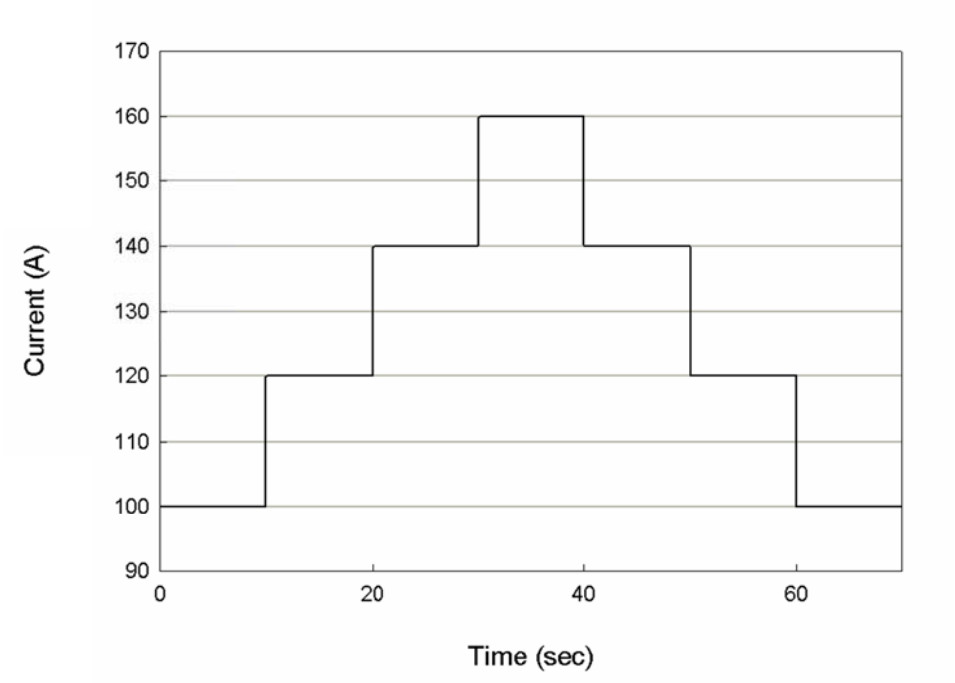

Figure 3-10. Current input for the simulation.

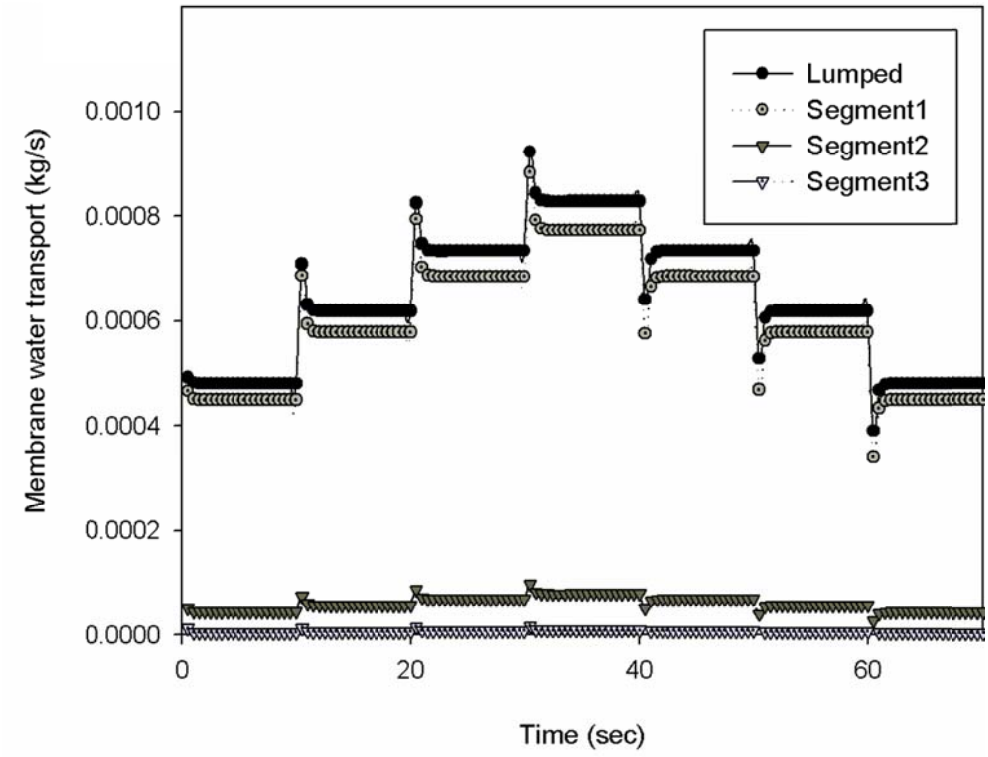

Figure 3-11. Comparison of the amount of water transport across the membrane between the lumped dynamic model and the data for the 3-segment dynamic model.

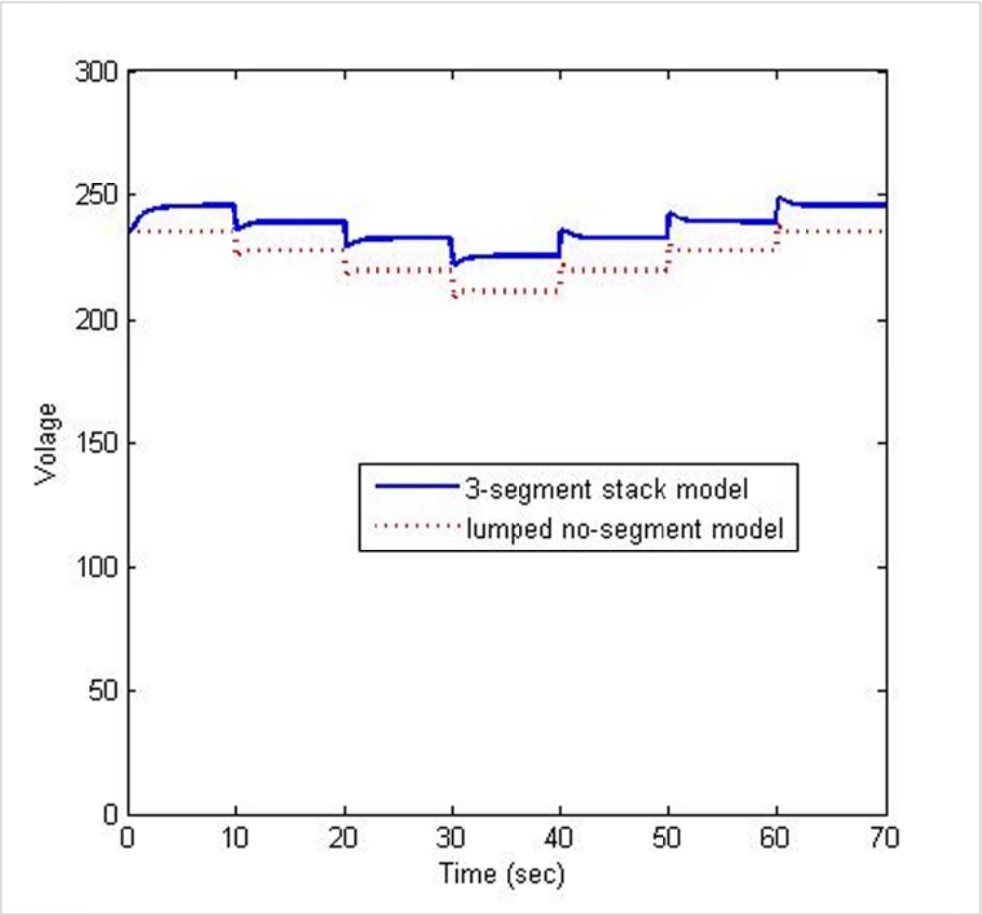

Figure 3-12. Terminal stack voltage in the lumped model and 3-segment model.

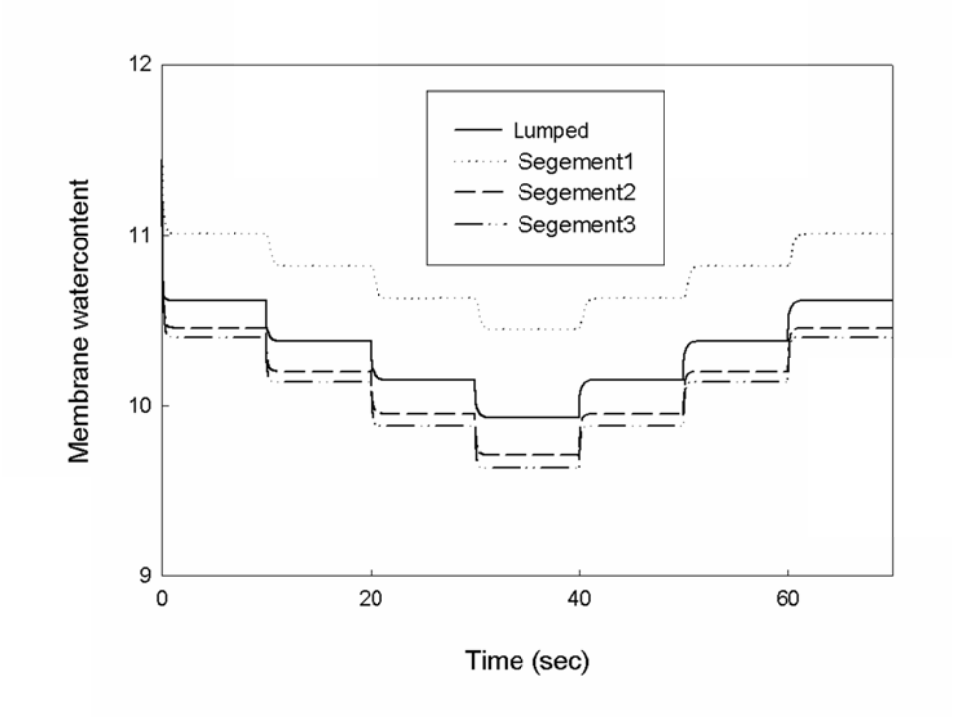

Figure 3-13. Water contents in the membrane region.

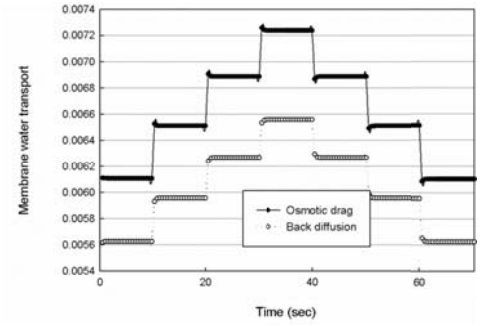

(a)

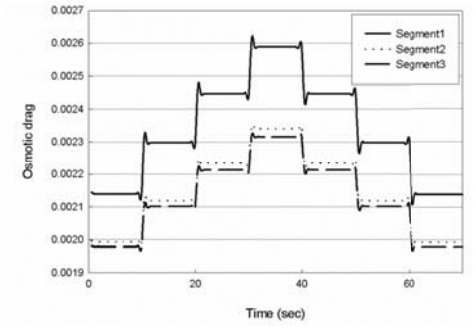

(b)

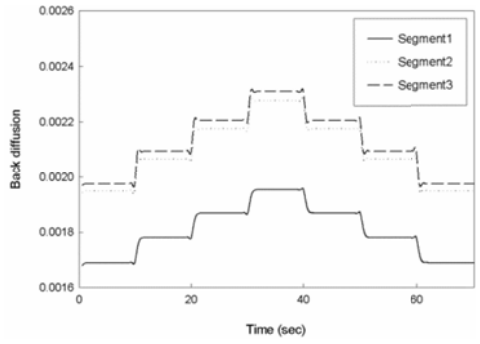

(c)

Figure 3-14. Water transport by osmotic drag and back diffusion: (a) the lumped model, (b) amount of osmotic drag in the 3-segment model, (c) Amount of back diffusion in the 3-segment model.

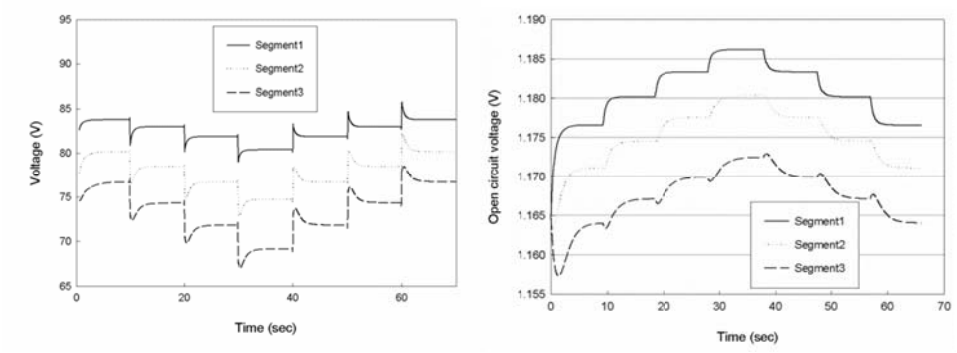

(a)

(b)

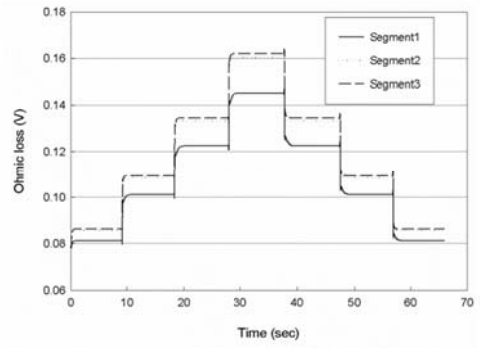

(c)

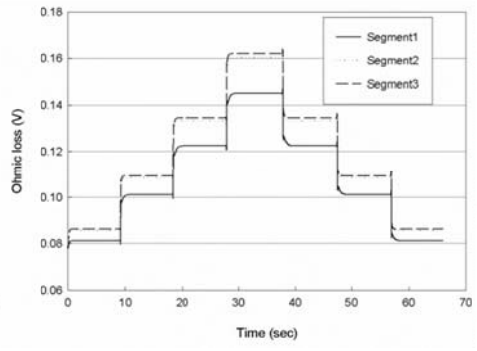

(d)

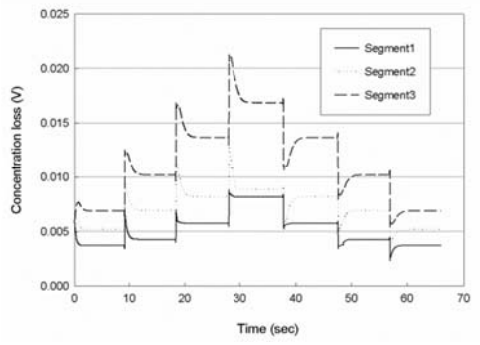

(e)

Figure 3-15. Voltage profile of the 3-segment model: (a) terminal voltage, (b) OCV, (c) activation , (d) ohmic loss, (e) concentration loss.

3.5. Conclusions

Proposed models have been applied to water content prediction. In the simulation of steady-state 2D rigorous model, solving algorithm based on FVM and SIMPLE is successfully conducted for calculating multiregional governing equations with single domain. This 2D model provides a detail distribution of water content in the cathode side. The analysis shows importance of vapor supplying at the low current density in the cathode inlet stream.

A PEM fuel cell stack model was investigated recently in dynamic modeling literature. Earlier studies have shown that the lumped dynamic stack model is challenging due to the simple application for the control strategy and optimization. A modified three-segment dynamic model, which can analyze the effect of water transport behavior on the stack performance with respect to the gas flow direction, was developed for a PEMFC stack system. The amount of liquid water transferred through the membrane in each segment was also calculated. Compared to the previous lumped dynamic model, the developed three-segment model can better estimate loss factors of the stack performance in each segment. This solution is important because water management in the PEMFC system may be important in real-time control applications or in cases of limited water supply, such as in fuel cell vehicles.

CHAPTER 4 : Modeling and Simulation of MCFC power plant for Monitoring System‡

4.1. Introduction

A Molten carbonate fuel cell (MCFC) power plant is an eco-friendly electricity generation system. Among several kinds of fuel cells for power plants using polymer electrolyte membrane fuel cells, such as solid oxide fuel cells and so on, MCFCs stand out as the most available technology for commercial release with respect to the cost and their capacity for electric energy generation. The advantages of an MCFC power plant are the absence of industrial noise and discernible cleanness, meaning that installation in downtown urban areas is possible. The main source of noise is mostly from the air blower. There are no air pollutants such as NOx and SOx; therefore, the MCFC system is the most promising technology that is close to commercialization.[29, 90-91]

In order to optimize design parameters, MCFC stack modeling was carried out.[92-93] These studies focused on the state estimation of the stack for understanding phenomena, i.e. effects of input parameters, temperature profiles on the stack. Research on analysis of MCFC systems also was demonstrated. Control strategies for a pilot scale power system were developed. Some studies of the pilot scale power system built mathematical models through experimentation, but the other studies developed similar mathematical models without employing

‡ The partial part of this chapter is taken from the author's published paper in journal.[89]

experimentation results.[28, 94-97] The performance of a combined MCFC system was investigated for a comprehensive thermodynamic analysis.[98]

The power generation system in an MCFC plant was developed by POSCO Energy, Inc. The specification of the commercialized MCFC power plant is summarized in Table 4-1. The plant's electric generating capacity is 330 kW maximum and decreases 5 kW every 6 months due to the stack degradation. The MCFC power plant primarily consists of three major units: a fuel processor, a stack, and electric power conditioning shown in Figure 4-1. The fuel processor is composed of a fuel pre-convertor, which reforms natural gas to hydrogen with a steam reforming reaction, and a heat recovery system to increase the overall system efficiency. In the fuel processor, Liquefied natural gas (LNG) with the primary treatment is mixed with steam through the humidifier, which removes the impurities in the desulfurizer and the particle filter. The LNG is then fed to the pre-convertor. The stack that generates the direct current is made up of hundreds of piled-up large cells, which are separated by bipolar plates. Details on the general stack and system are reported in the literature.[99-100]

The MCFC power plant is composed of the stack and the balance of plant (BOP), which is commonly divided into the electrical BOP and the mechanical BOP. Each component has dozens of sensors that typically estimate the temperature, flow rate, and pressure. Due to an overabundance of sensors, false alarms occur quite frequently and simultaneously. Both batch and continuous systems have many single variables. Simple monitoring system only detects abrupt faults. Complicated faults involving interlock control system and drift of multiple variables are not detected.[101-102] For this reason, an advanced monitoring system for a plant size

system should be considered. In this chapter, we present a multivariate statistical monitoring system, considering the performance of fault detection with various variable groups, based on the principal component analysis technique.

Table 4-1. Summary of the specification for the MCFC power plant

Item	Specification
Power Output	300 kW
Total fuel consumption (LNG@LHV 9,500 Kcal/Nm^3)	58Nm^3/hr
Plant efficiency	47±2%@ISO
Exhaust gas temperature	343℃
Exhaust gas pressure	127 mmH_2O

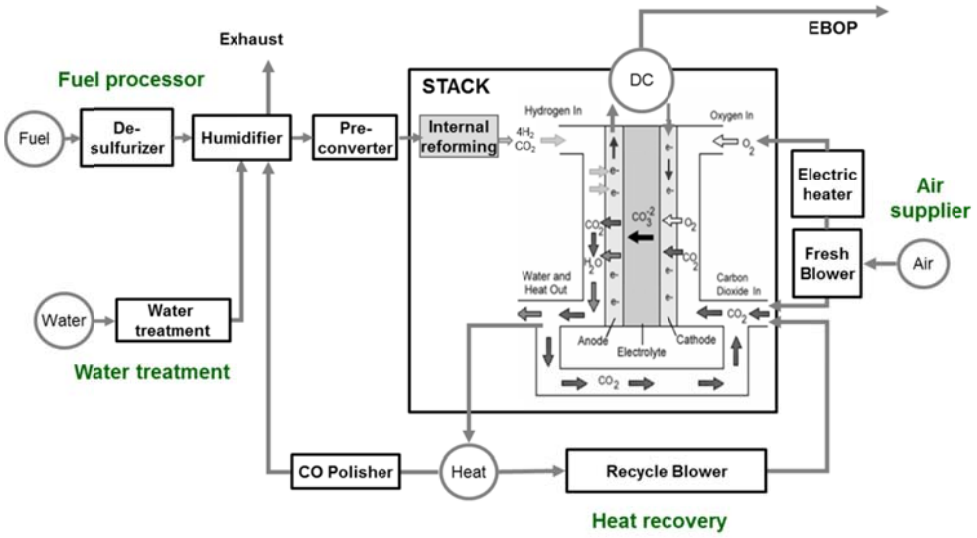

Figure 4-1. Schematic diagram of the MCFC system.

4.2. Methodology for process monitoring

The most well-known traditional monitoring technique for a chemical process is the statistical process control (SPC) method. The main purpose of this method is to monitor the performance of the process fundamentally observing whether the state of the process is in control. The state of control is defined as having certain variables remain close to their desired values and the only source of variation being a common cause, i.e. process disturbance and set points change. This traditional method has been used for guiding safe and stable operations, which leads to qualified products by eliminating the cause or improving the operating procedures.[102]

There are different types of univariate charts for SPC such as Shewhart, Cumulative sum (CUSUM), or Exponentially weighted moving average (EWMA), which are used for monitoring key product variables in order to detect the occurrence of any event. Since the SPC method uses a chart for a small number of variables only, this approach is inappropriate for most industrial processes. In modern process industries, massive amounts of reciprocal data such as temperature, pressure, and flowrate are collected at one second intervals. All these process variables should be used to assess the operating performance in a monitoring and diagnostic scheme.[101]

Multivariate statistical projection methods extract effective information from all the variables while considering the correlation of the process variables by providing a reduction in the dimensions. A popular method for reducing the dimensionality of process variable space is Principal component analysis (PCA).[103]

4.2.1. Principal component analysis for fault detection

PCA estimates the loading vectors, which are ordered by the amount of variance explained. The training data matrix $X(n\times m)$, which has n observations of m measurement variables, can be decomposed to produce loading vectors by using Singular value decomposition (SVD).

$$\frac{1}{\sqrt{n-1}}X = U\sum V^T \tag{4-1}$$

where $U(n\times n)$ and $V(m\times m)$ are unitary matrices and diagonal matrix $\sum(n\times m)$ contains nonnegative real singular values.

The normal operating condition can be defined by Hotelling's T.[2]

$$T_\alpha^2 = \frac{\left(n^2-1\right)}{n\left(n-a\right)}F_\alpha\left(a, n-a\right) \tag{4-2}$$

where a is the number of selected Principal components (PCs), $F_\alpha(a,n-a)$ is the upper 100α% critical point of the F-distribution with a and n-a degrees of freedom. If the value of T^2 statistic is greater than the threshold given by Equation (4-2), it indicates that a fault has occurred.

For the residual portion, the lowest m-a singular values, can be monitored using the Q statistic.

$$Q = r^T r, r = \left(I - PP^T\right)X \tag{4-3}$$

where r is the residual vector.[104]

The resulting lower dimensional models have been successively applied to detect abnormal process operations.[105-107]

The general procedure for building up a monitoring system is shown in Figure 4-2.

In the following, the details of the PCA modeling step is introduced in order to decide which variable groups performed well followed by data preprocessing. In the next section, a summary of the process description and multivariate monitoring architecture are given, followed by a detailed summary of the variable selection method.

4.2.2. Heuristic recursive variable selection algorithm

The monitoring architecture starts with the multivariate statistical monitoring technique, e.g. PCA. Details for the equations used in PCA modeling are described elsewhere.[108] Results of the PCA modeling with all variables are shown in Figure 4-3. The Score plot represents the overall status of the system operation in a two-dimensional space, where the outer circle is the statistical control limit. Each dot point represents a process status in the score plot. If a dot point crosses the control limit, the process operation is in an abnormal situation. In the PCA modeling step, performance criteria of the method are representative performance and the cumulative sum of explained variance. Representative performance can be easily checked in the score plot. Figure 4-3 shows the case that conventional PCA does not work for real processes. Although regarded as normal data set, a copious number of score points are projected outside the control limit in the score plot. Criterion of the cumulative sum of explained variance is at least greater than 70% for principal component 1 (PC1) and principal component 2 (PC2). The cumulative sum of the explained variance is 55% of PC1 (44%) and PC2 (11%) in Figure 4-3. Results of conventional PCA did not satisfy both performance criteria. In order to improve the monitoring performance, an appropriate variable selection method has to be implemented to eliminate useless variables.

For the first step of data preprocessing, heuristic recursive variable selection method based on factor analysis was considered. Factor analysis is one of the data compression techniques for extracting information with intrinsic order. In order to decompose three-way data matrix (batch × variable × time) of batch process, parallel factor analysis was adopted.[109] In the monitoring for environmental quality of fresh water, factor analysis was used for exploring the specific characteristic of information.[110] In addition, factor analysis can be used to determine how many variable groups are presented in all-variable sets. Factor analysis is typically used to explain the correlation among variable groups whereas PCA focuses on explaining the variability of the variable groups. Figure 4-4 shows a scheme of the heuristic recursive variable selection architecture. First, the criteria for going back to the variable update step occurs when the cumulative sum of the explained variance is less than 80% with two principal components, along with the eigenvalue of each principal component being less than 1. When the criteria were satisfied, comparison with PCA models from other variable sets for factor validation was performed. If these criteria were not satisfied, variable update was performed. In this step, factor analysis suggested variable groups that were physically correlated with a specific region of the process, i.e. fuel processor and heat recovery subsystem. An example of factor analysis is presented in Table 4-2. Factor analysis rearranges the variables in a descending order of standardized scoring coefficients for grouping variables that are located in the similar region of the process. For example, in factor 1, same group variables such as temperature 1, temperature 2, pressure 1 and flowrate 1 were located in the cathode region. Each

variable group was verified by comparing with the actual sensor location in the same region of the process, using P&ID, operator interview, etc.

The error rate was calculated for the validation of monitoring performance. In the validation step, trip event data were used for checking the score plot and the squared prediction error with the upper critical limit (UCL). This result was compared with the univariate alarm history and monitoring results. Finally, two new groups (group 2, group 3) of variables were determined by heuristic method. Figure 4-5 shows that group 3 performed well on a set of normal status because almost all points were bounded in the limit. The cumulative sum of the explained variance is 76%.

In the Section 4-4, these new variable sets were compared with the base group and a conventionally selected variable set, named group 1. Up to and including the 19^{th} variable, ranked by the proportion of PCA loading, was used for group 1. Selected variables are stack temperature sensors, stack current sensors, fuel pressure sensor and so on. In addition, the 19 variables were also the same number of variables used in group 3, which was determined by the heuristic architecture.

Table 4-2. Example of the standardized scoring coefficients of the factor analysis

Variables	Standardized Scoring Coefficients	
	Factor 1	Factor 2
Temperature 1	0.08073*	0.02249
Pressure 1	0.08010*	0.01201
Temperature 2	0.07986*	0.01769
Flowrate 1	-0.06259*	-0.07006
Temperature 3	-0.01911	0.12508**
Flowrate 2	0.04552	0.9898**

*, ** denotes including same groups.

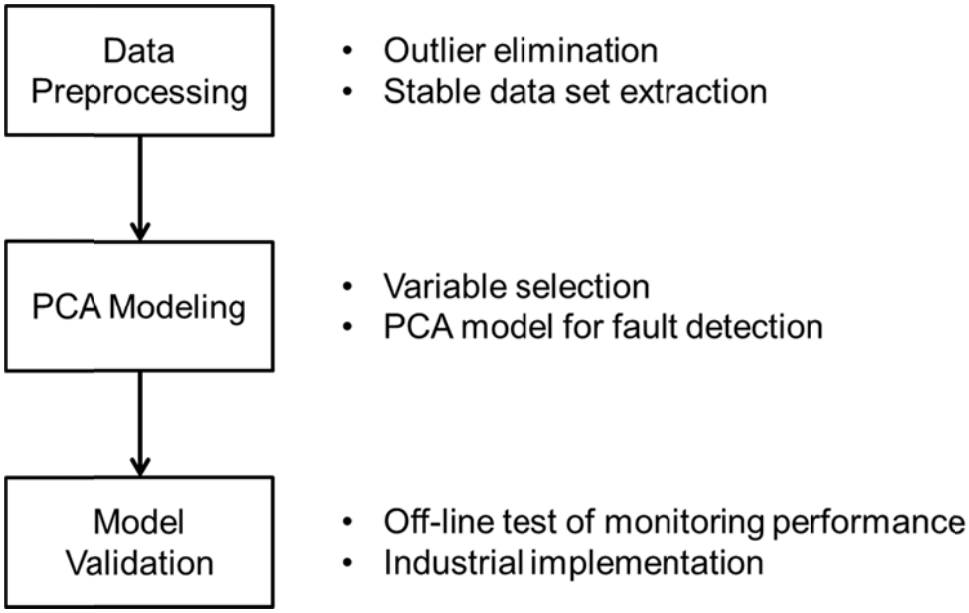

Figure 4-2. General procedure for PCA modeling for multivariate monitoring.

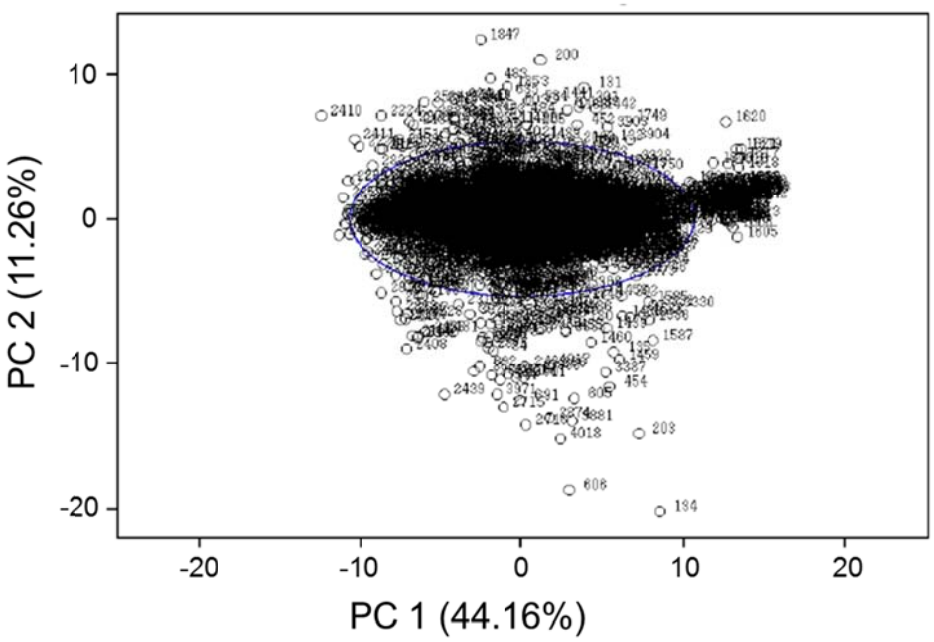

Figure 4-3. PCA score plot for all-variable groups with normal operations data.

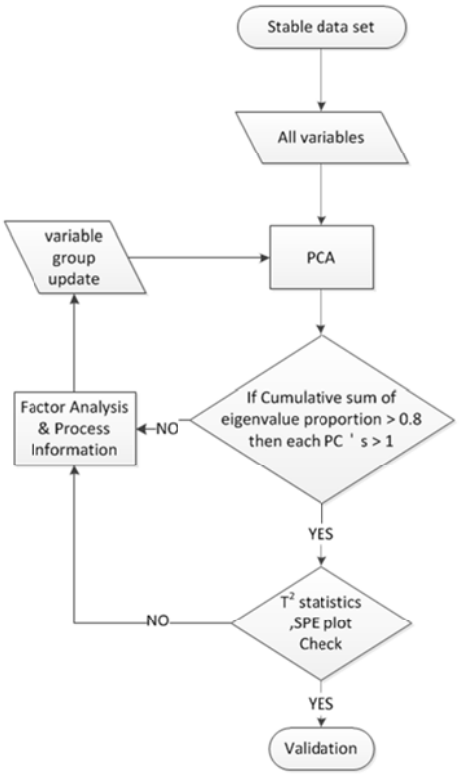

Figure 4-4. Flow chart of the heuristic variable selection method for the MCFC power plant.

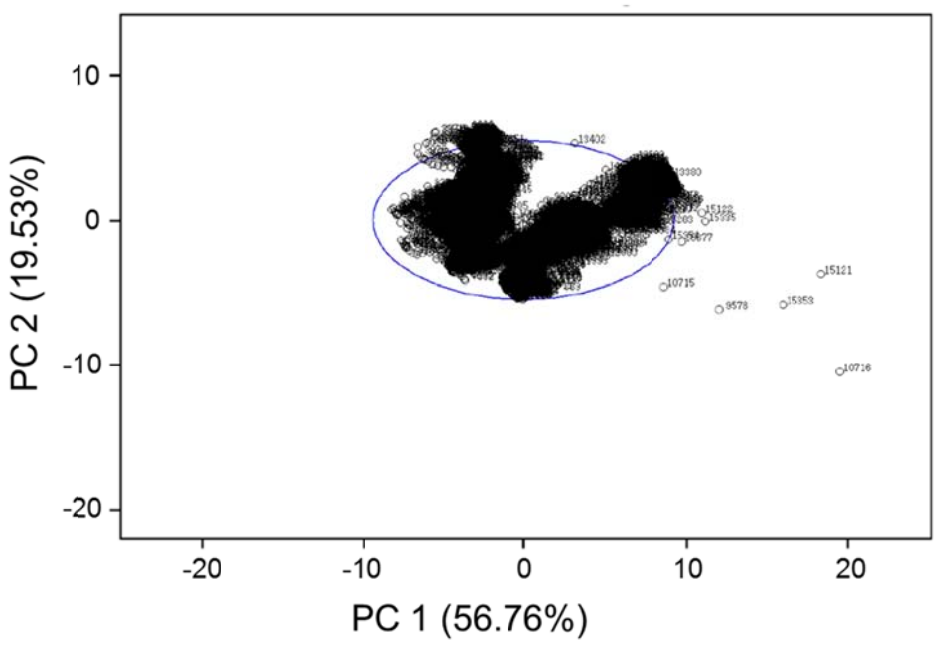

Figure 4-5. PCA score plot for the 19-variable group after variable selection with normal operations data.

4.3. Implementation to MCFC power plant

The PCA technique described in Section 4-2 provides the basis of design a multivariate monitoring system. In order to conduct off-line test for real plant data, data preprocessing and validation are necessary. In the simulation studies, process variables are not frequently changed[111-112]; otherwise, real operations data may have noise and abrupt change that is due to sensing errors.[113]

The present monitoring system installed in the MCFC power plant has limited sensing capability in the same way as the univariate statistical technique. For the off-line analysis of the monitoring performance, real operations data and trip history were collected for 6 months in 2009. Note that the power plant was running in the similar mode during the data collection albeit an approximate 5 kW decrease in the power capacity occurred once. Alternative-current generation and tagged ACKW (alternative current kilowatt) during the collected period are shown in Figure 4-6.

There are hundreds of measurements from the sensors. The operations data were measured on average for one minute at the distributed control system (DCS). Since time order of system dynamics is slow except for that related to the electric power conditioning, minute-average data were sufficient to carry out the off-line tests. According to the history of system trips recorded by field operators, 9 trips were selected to test the monitoring performance of fault detection. When cells in stack normally generate similar amount of electric direct current, the status of system is deemed normal thus characterized as being cell balanced. Some faults are related to the breaking of cell balance, which causes the outlet temperature increment of the cathode. Root cause for unintended system shut down and reset could not be

substantiated. To develop the PCA model, normal operations data for 16810 minutes were used. To validate the monitoring performance, 18 cases of operations were selected, which consisted of 9 fault cases and 9 normal cases. After extracting the trip cases, the ACKW of the normal operations data is shown in Figure 4-7.

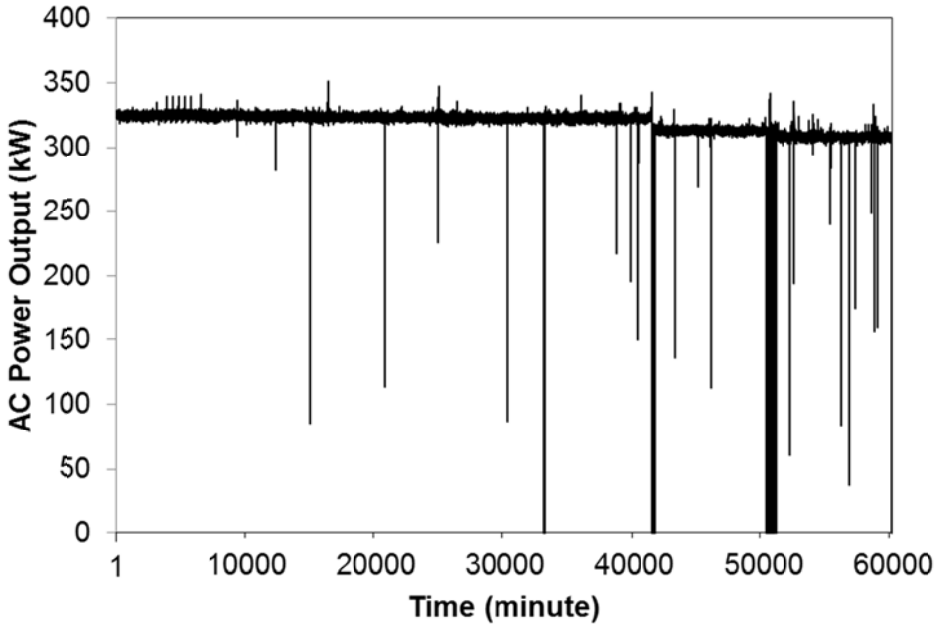

Figure 4-6. Electric AC power generation during 6 months of data collection.

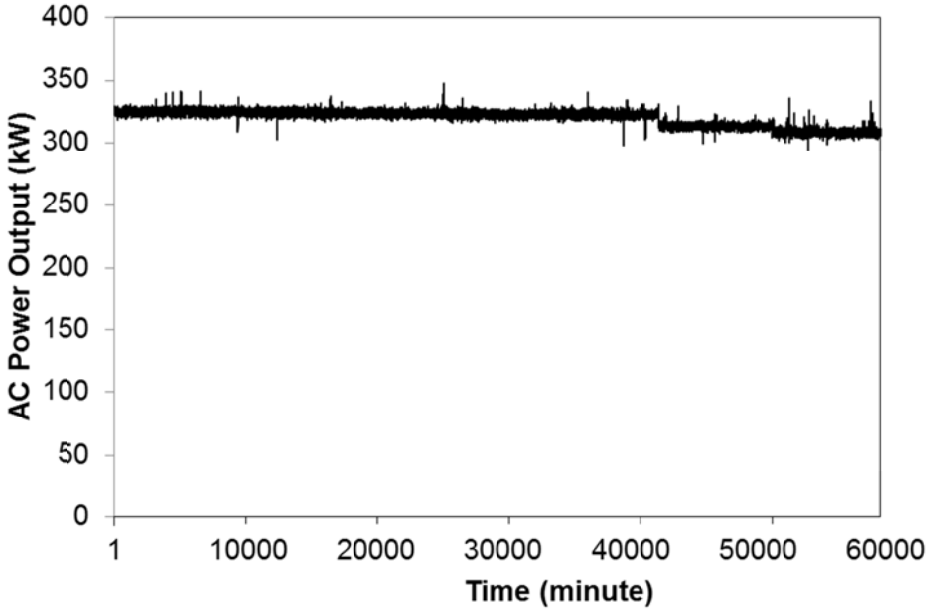

Figure 4-7. Electric AC power generation after eliminating the trip periods during 6 months of data collection.

4.4. Results and discussion

First, the off-line monitoring results are presented for the fault detection performance, from the plant operations data, along with the trip history. Subsequently, the comparison result with other variable groups were reported in order to validate the improvement in the monitoring performance in terms of type I and type II error rates[114]:

$$\text{Type I error rate} = \frac{\text{False positive cases}}{\text{All normal cases}} \tag{4-4}$$

$$\text{Type II error rate} = \frac{\text{False negative cases}}{\text{All trip cases}} \tag{4-5}$$

where false positive refers to the cases in which a normal process status is incorrectly identified whereas false negative means the inability to detect an actual fault situation.

Figure 4-8 shows no abnormality in the T^2 plot with all variables or the selected variables. For normal operation data, all points were bounded in dashed line of limit with both T^2 plots. T^2 plot is commonly used to show the occurrence of a fault. If a process malfunction changes the correlation structure among the monitored variables, the score chart and T^2 plot are no longer valid. Therefore, the T^2 value will remain within the control limits; however, the Q statistic will move outside the UCL. As mentioned in Section 4.2, the Q statistic represents the residual portion of the reduced dimension data. Figure 4-9 shows the base group is not valid for normal operations data to identify nominal system status. However, the Q statistic of group 3 can represent that the PCA model is valid in the normal system status shown in Figure 4-9.

The result of the off-line test for the trip case is shown in Fig 4-10. At 77 minutes, which is the last point of the plot, the system mode is changed to trip. If the monitoring system cannot detect when the system status goes to fault, the Q statistic value remains within the UCL, e.g. the false negative case. However, when the monitoring system works well with early fault detection, the Q statistic value exceeds the UCL before the system mode changes. The comparison results with the various variable groups are presented in Table 4-3.

Type I error means that a false alarm has occurred when the system status is normal, whereas type II error represents the failure to detect the fault. In the base case, both type I and type II error rates were greater than 50%. As the number of variables is decreased, the false alarm is decreased in the group 2 while the type II error rate increased. Since the number of variables decreased, variables that were not helpful in monitoring the process during normal operation were eliminated; however, these variables also contain important information for the early detection of evidence for system faults. With the heuristic method for variable selection, results of both group 2 and group 3 improve the monitoring performance. Especially, in the result of group 3, the error rates for type I and type II were reduced more than half of the error rates that occur in the base case. The cumulative sum of explained variance is also increased from 65% base group to 76% group 3. It means the heuristic architecture can provide an appropriate means for variable selection.

Table 4-3. Comparison of type I and type II error rates with the reference and modified models

Error rate (%)		Base group 72 variables	Group 1 19 variables by PCA loading	Group 2 63 variables by heuristic method	Group 3 19 variables by heuristic method
Q statistic	Type I	55	11	22	11
	Type II	77	88	44	22

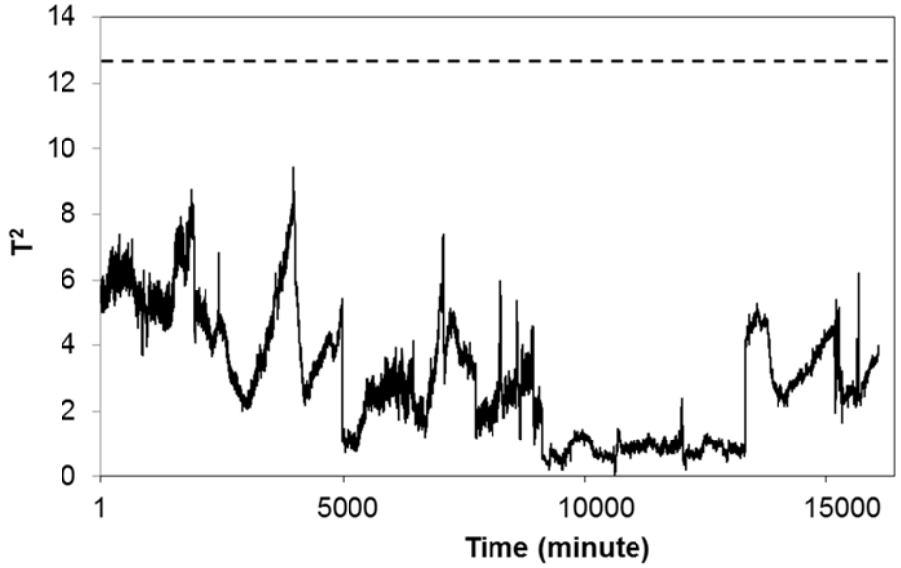

(a)

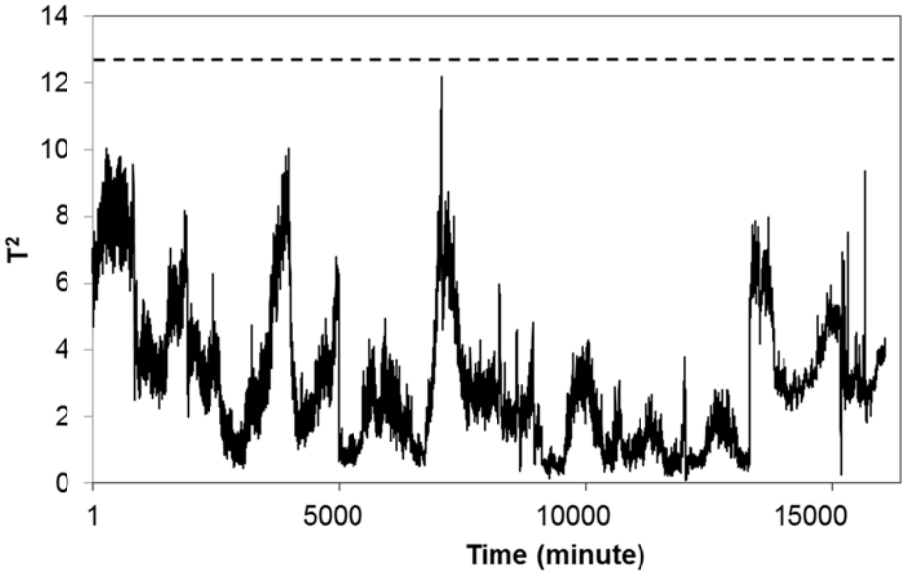

(b)

Figure 4-8. Monitored T^2 plot of the normal operations data: (a) all-variable group (b) 19-variable group.

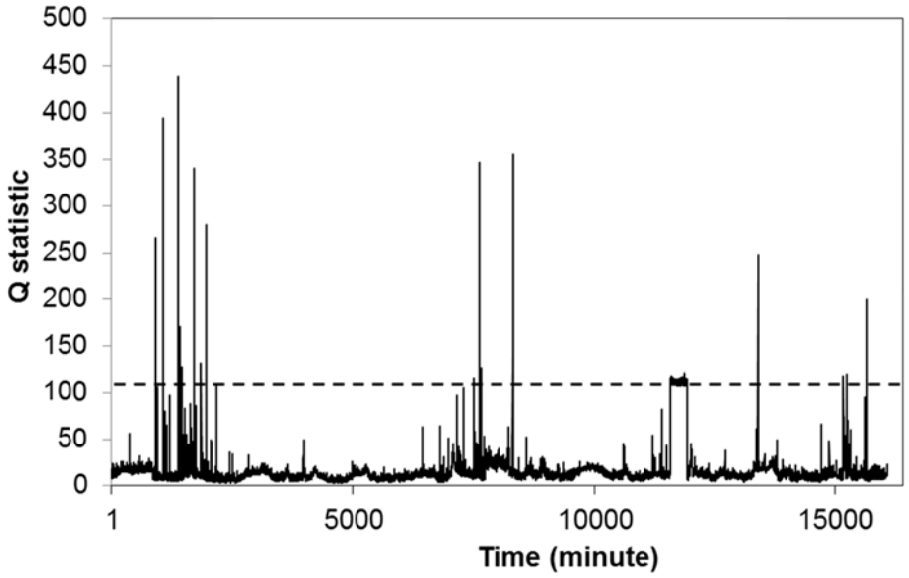

(a)

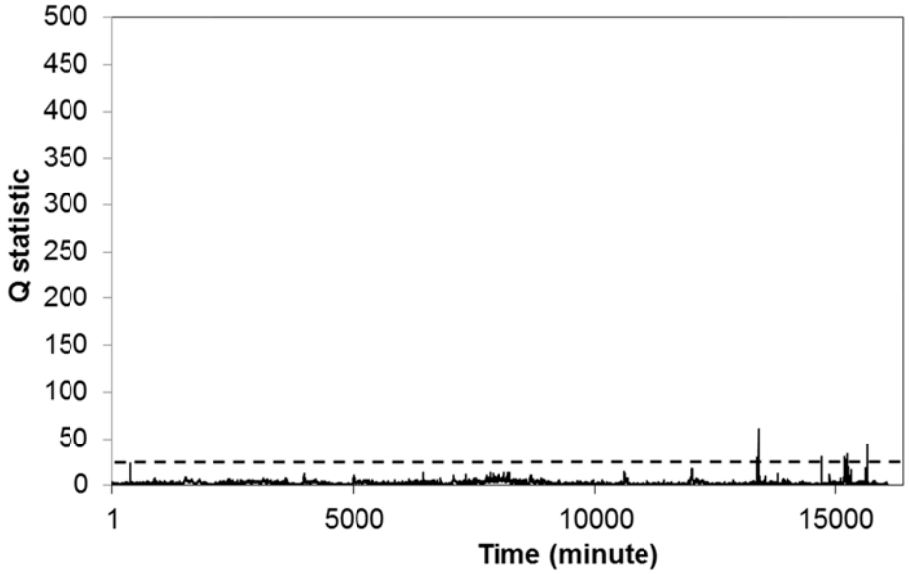

(b)

Figure 4-9. Monitored *Q* statistic plot of the normal operations data: (a) all-variable group (b) 19-variable group.

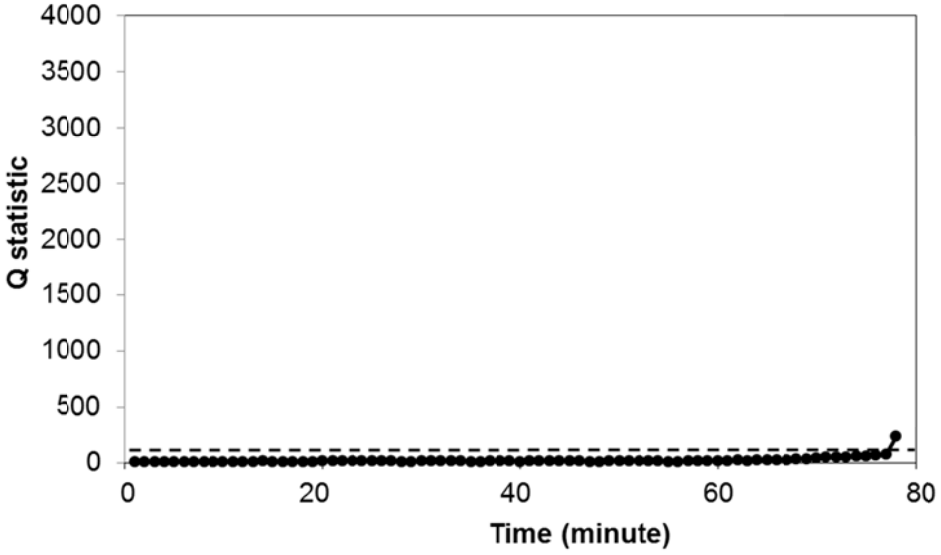

(a)

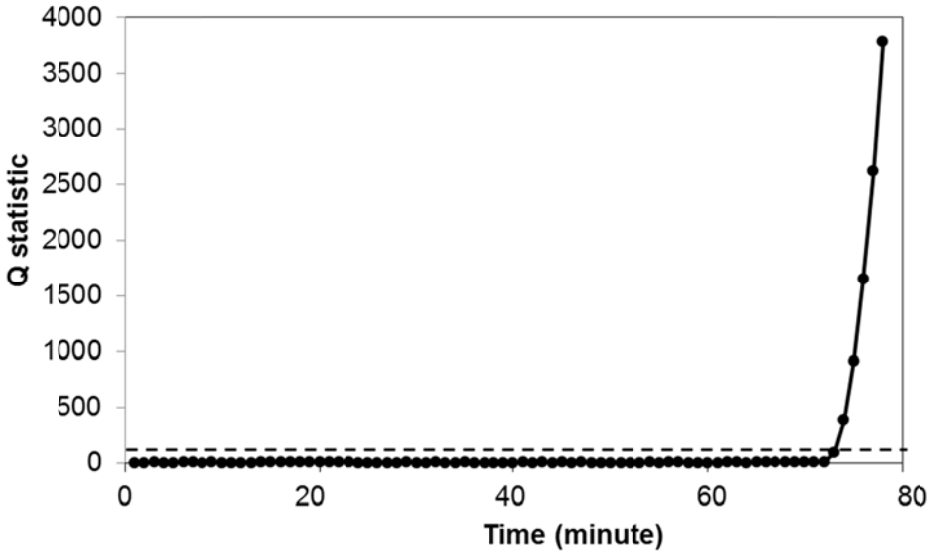

(b)

Figure 4-10. Monitored Q statistic plot of the trip data: (a) all-variable group (b) 19-variable group.

4.5. Conclusions

In this chapter, off-line analysis for the performance estimation of a multivariate monitoring system in a MCFC power plant is carried out. In terms of development, the basic PCA model cannot work for all the variables since all 163 variables cannot represent the system status well. In order to implement an advanced monitoring technique for the commercialized process, a heuristic recursive variable selection method for PCA modeling is developed. The comparison results of the 4 variable groups are reported. When comparing type I and type II errors, the proposed method demonstrates improvement in monitoring performance whether the system status is normal or in trip mode. The multivariate monitoring system based on PCA modeling is inspired by the variable selection method. The proposed method offers several advantages. First, the equation of the PCA model to estimate the monitoring index, e.g. score, T^2, and Q statistic, is simple; therefore, it may be easily implemented to existing monitoring systems. Second, the reduced dimension space appears to be more understandable to the operator in terms of the overall system. To prevent a system trip situation, on-line diagnostic tools based on the PCA model can be implemented for the advanced monitoring system.

CHAPTER 5 : Concluding Remarks

5.1. Conclusions

The objective of this thesis is to propose the purpose oriented modeling and simulation in the fuel cell system. In order to satisfy the purpose of study, proper level of modeling methods such as lumped model, rigorous model and statistic model is needed. Two kinds of steady-state model, one dynamic model and one statistic model are used through the thesis.

In this thesis, four kinds of model for two types of fuel cell system are proposed. The purpose of modeling is three, which are economic feasibility analysis, understanding transport phenomena, improving monitoring performance. First, a process model for the PEMFC power plant is developed and simulated. The purpose of process model development is assessed economic feasibility of the PEMFC power plant using by-product hydrogen within political and technical scenarios. An economic advantage of using by-product hydrogen is proved by comparable case studies. Under present technical level, the PEMFC power plant has no economic profitability. Therefore, in the case studies, a necessity of advanced technical development and supporting system by the government is proposed. Second, a steady-state model for a single cell and a dynamic model for a stack are developed and simulated. In order to estimate detail distribution of water content in the channel and the membrane, the rigorous two-dimensional model are presented. Solving algorithm for simulation is suggested. The result is validated with experimental data from a single cell experiment. Analysis of a single cell shows the depletion of water vapor under the low current condition. The lumped

dynamic model is modified to provide more detail distribution of water content and performance loss factor in the stack. The modified 3-segment model is suggested with pressure assumption and modeling of cathode outlet manifold. As the current increased, concentration loss by back diffusion is increased. At the exit region of stack, water content in the membrane is enough to transfer proton through membrane. In order to considering water management in the stack, performance predictor is required. Third, a statistic model for monitoring system of the MCFC power plant is presented. In order to improve fault detection performance, heuristic variable selection method based on factor analysis and principal component analysis is suggested. The result is validated with operation data and trip history from a 300kW MCFC power plant installed in the Pohang in South Korea. The error rate of type I, II is decreased by using proposed variable selection method.

In the development of modeling and simulation, various tools such as excel spread sheet, Visual C++, MATLAB/Simulink and SAS are conducted. In order to analyze economic feasibility, excel spread sheet is enough to solve the process model and to estimate economic assessment. Coding using Visual C++ is needed to solve multiregional governing equation set by using own solving algorithm for a rigorous model. In order to simulate dynamic model, MATLAB/Simulink provides useful functions with time variation. Because of lumped model has no complication of solving equations, toolbox for solving ordinary differential equation in the MATLAB works well. In order to handle a huge amount of process operation data, MATLAB or SAS among commercial packages are more suitable than spread sheet when monitoring method is based on PCA. These descriptions of simulation tool implied that proper modeling and simulation uses appropriate tools.

These proposed methods of modeling and simulation are applied for completing each purpose. This thesis describes many kinds of modeling and simulation in the fuel cell system as an example of model selection.

5.2. Future works

In this thesis provides a part of modeling and simulation in two types of fuel cell system. In order to commercialize a fuel cell system, further researches and verifications are required. Following works are needed to accomplish implementation. For the transport application of PEMFC, dynamic modeling and simulation is required to construct control strategy under various operating conditions. Since the objective of the proposed steady-state and dynamic model is focused on understanding transport phenomena, dynamic modeling and simulation for solving control problem is needed to quick response for vehicle requirement. For the stationary application of MCFC power plant, advanced fault diagnosis methods such as Fisher discriminant analysis (FDA), Support vector machine (SVM) can be used for rapid and precise diagnosis. In order to prevent system shut down, fault prognosis is needed to in advance manage of process operation.

Nomenclature

a_i	activity
c_f	fixed charge concentration
c_i	concentration (mole l^{-1})
D_i	diffusivity (cm2 s^{-1})
E_Φ	electrical potential (V)
F	Faraday constant (96,485 C mol^{-1})
F_i	fuel consumption rate (L min^{-1})
H	water content ratio
H_i	operation hour (hour)
i	cell operating current density (A cm^{-2})
j	exchange current density (A cm^{-3})
m	mass flow rate (g min^{-1})
P	pressure (atm)
P_i	power demand (kW)
p	partial pressure (kPa)
R	molar gas constant (8.314 J mol^{-1} K^{-1})
S	source term
T	temperature (K)
u	x-axis velocity (m s^{-1})
V	humid volume per mass (m^3 kg^{-1})
v	y-axis velocity (m s^{-1})

X	molar fraction of liquid
Y	molar fraction of gas

Greek letters

ε	porosity
η	electrode overpotential (V)
λ	water content (mol H_2O mol $-SO_3H^{-1}$)
v	volumetric flow rate (L min^{-1})
σ_m	proton conductivity in the membrane (Ω^{-1} m^{-1})
ρ	H_2 density at average temperature (kg m^{-3})
μ	viscosity (g cm^{-1} s^{-1})
Φ	relative humidity (%)
E_{Φ}	potential (V)

Subscripts

0	initial value
a	anode
c	cathode
i j	species i, j
in	channel inlet flow
m	membrane
out	channel outlet flow
w	vapor H_2O

Abbreviations

ACKW	Alternative current kilowatt
ADG	Anaerobic digester gas
BOP	Balance of plant
CER	Certified emission reduction
CHP	Combined generation of heat and power
COE	Cost of electricity
CRF	Capital recovery factor
CUSUM	Cumulative sum
DCS	Distributed control system
DOE	Department of energy, USA
EUA	EU carbon dioxide allowance
EWMA	Exponentially weighted moving average
FDA	Fisher discriminant analysis
FVM	Finite volume method
GDL	Gas-diffusion layers
HHV	High heating value
LHV	Low heating value
LNG	Liquefied natural gas
MACRS	Modified accelerated cost recovery system
MCFC	Molten carbonate fuel cell
NG	Natural gas
NPV	Net present value
O&M	Operation and maintenance

OCV	Open circuit voltage
PAFC	Phosphoric acid fuel cell
PC	Principal component
PCA	Principal component analysis
PEMFC	Proton exchange membrane fuel cell
PSA	Pressure swing adsorption
R&M	Repair and maintenance
RH	Relative humidity
SECA	Solid state energy conversion alliance
SIMPLE	Semi-implicit method for pressure linked equation
SMP	Sale marginal price
SOFC	Solid oxide fuel cell
SPC	Statistical process control
SVD	Singular value decomposition
SVM	Support vector machine
UCL	Upper critical limit

Literature cited

1. Mitsos, A.; Palou-Rivera, I.; Barton, P. I., Alternatives for micropower generation processes. Industrial & engineering chemistry research 2004**,** 43 (1), 74-84.
2. Wu, S.; Kotak, D.; Fleetwood, M., An integrated system framework for fuel cell-based distributed green energy applications. Renewable Energy 2005**,** 30 (10), 1525-1540.
3. Cheddie, D.; Munroe, N., Review and comparison of approaches to proton exchange membrane fuel cell modeling. Journal of power sources 2005**,** 147 (1), 72-84.
4. Sopian, K.; Wan Daud, W. R., Challenges and future developments in proton exchange membrane fuel cells. Renewable Energy 2006**,** 31 (5), 719-727.
5. Mitsos, A.; Chachuat, B.; Barton, P. I., What is the design objective for portable power generation: Efficiency or energy density? Journal of power sources 2007**,** 164 (2), 678-687.
6. Xue, D.; Dong, Z., Optimal fuel cell system design considering functional performance and production costs. Journal of power sources 1998**,** 76 (1), 69-80.
7. Bernay, C.; Marchand, M.; Cassir, M., Prospects of different fuel cell technologies for vehicle applications. Journal of power sources 2002**,** 108 (1-2), 139-152.
8. Roy, R.; Colmer, S.; Griggs, T., Estimating the cost of a new technology intensive automotive product: A case study approach. International Journal of Production Economics 2005**,** 97 (2), 210-226.
9. De Bruijn, F., The current status of fuel cell technology for mobile and stationary applications. Green Chemistry 2005**,** 7 (3), 132-150.
10. Aki, H.; Yamamoto, S.; Kondoh, J.; Maeda, T.; Yamaguchi, H.; Murata, A.; Ishii, I., Fuel cells and energy networks of electricity, heat, and hydrogen in residential areas. International Journal of Hydrogen Energy 2006**,** 31 (8), 967-980.
11. Acres, G. J. K., Recent advances in fuel cell technology and its applications. Journal of power sources 2001**,** 100 (1), 60-66.
12. Ishikawa, T.; Yasue, H., Start-up, testing and operation of 1000 kW class MCFC power plant. Journal of power sources 2000**,** 86 (1-2), 145-150.
13. Silveira, J. L.; Martins Leal, E.; Ragonha, L. F., Analysis of a molten carbonate fuel cell: cogeneration to produce electricity and cold water. Energy 2001**,** 26 (10), 891-904.
14. Bischoff, M.; Huppmann, G., Operating experience with a 250 kW molten carbonate fuel cell (MCFC) power plant. Journal of power sources 2002**,** 105 (2), 216-221.
15. Bischoff, M., Molten carbonate fuel cells: a high temperature fuel cell on

the edge to commercialization. Journal of power sources 2006, 160 (2), 842-845.
16. Hendry, C.; Harborne, P.; Brown, J., Niche entry as a route to mainstream innovation: learning from the phosphoric acid fuel cell in stationary power. Technology Analysis & Strategic Management 2007, 19 (4), 403-425.
17. Amphlett, J. C.; Baumert, R.; Mann, R. F.; Peppley, B. A.; Roberge, P. R.; Harris, T. J., Performance modeling of the Ballard Mark IV solid polymer electrolyte fuel cell. Journal of the Electrochemical Society 1995, 142, 1.
18. Fowler, M. W.; Mann, R. F.; Amphlett, J. C.; Peppley, B. A.; Roberge, P. R., Incorporation of voltage degradation into a generalised steady state electrochemical model for a PEM fuel cell. Journal of power sources 2002, 106 (1), 274-283.
19. Barbir, F.; Yazici, S., Status and development of PEM fuel cell technology. International Journal of Energy Research 2008, 32 (5), 369-378.
20. Wang, Y.; Chen, K. S.; Mishler, J.; Cho, S. C.; Adroher, X. C., A review of polymer electrolyte membrane fuel cells: Technology, applications, and needs on fundamental research. Applied Energy 2011, 88 (4), 981-1007.
21. Stambouli, A. B.; Traversa, E., Solid oxide fuel cells (SOFCs): a review of an environmentally clean and efficient source of energy. Renewable and Sustainable Energy Reviews 2002, 6 (5), 433-455.
22. Wang, X.; Huang, B.; Chen, T., Data-driven predictive control for solid oxide fuel cells. Journal of Process Control 2007, 17 (2), 103-114.
23. Ma, Y.; Karady, G. G.; Winston III, A.; Gilbert, P.; Hess, R.; Pelley, D., Economic feasibility prediction of the commercial fuel cells. Energy Conversion and Management 2009, 50 (2), 422-430.
24. Staffell, I.; Green, R., Estimating future prices for stationary fuel cells with empirically derived experience curves. International Journal of Hydrogen Energy 2009, 34 (14), 5617-5628.
25. Bove, R.; Lunghi, P., Experimental comparison of MCFC performance using three different biogas types and methane. Journal of power sources 2005, 145 (2), 588-593.
26. Krumbeck, M.; Klinge, T.; Döding, B., First European fuel cell installation with anaerobic digester gas in a molten carbonate fuel cell. Journal of power sources 2006, 157 (2), 902-905.
27. Peppley, B. A., Biomass for fuel cells: a technical and economic assessment. International journal of green energy 2006, 3 (2), 201-218.
28. Marra, D.; Bosio, B., Process analysis of 1 MW MCFC plant. International Journal of Hydrogen Energy 2007, 32 (7), 809-818.
29. Moreno, A.; McPhail, S.; Bove, R., International Status of Molten Carbonate Fuel Cell (MCFC) Technology. ENEA–Communication Unit, Roma 2008.
30. Biyikoglu, A., Review of proton exchange membrane fuel cell models. International Journal of Hydrogen Energy 2005, 30 (11), 1181-1212.
31. Jeong, H.; Cho, S.; Han, C., Economic feasibility analysis of a PEMFC

power plant fueled by by-product hydrogen from a petrochemical complex with a pressure swing adsorption unit. Journal of Chemical Engineering of Japan 2012, On-line published.
32. Kim, D.; Jeong, C.; Han, C., Economic Efficiency of Using Existing Pipe Line in Hydrogen Network. Korean Chemical Engineering Research 2008**,** 46 (3), 598-603.
33. Jeong, C.; Han, C., Byproduct Hydrogen Network Design Using Pressure Swing Adsorption and Recycling Unit for the Petrochemical Complex. Industrial & engineering chemistry research 2011.
34. Bar-On, I.; Kirchain, R.; Roth, R., Technical cost analysis for PEM fuel cells. Journal of power sources 2002**,** 109 (1), 71-75.
35. Wallmark, C.; Alvfors, P., Technical design and economic evaluation of a stand-alone PEFC system for buildings in Sweden. Journal of power sources 2003**,** 118 (1-2), 358-366.
36. Jiang, Z.; Gao, L.; Blackwelder, M. J.; Dougal, R. A., Design and experimental tests of control strategies for active hybrid fuel cell/battery power sources. Journal of power sources 2004**,** 130 (1-2), 163-171.
37. Kamarudin, S.; Daud, W.; Md Som, A.; Takriff, M.; Mohammad, A., Technical design and economic evaluation of a PEM fuel cell system. Journal of power sources 2006**,** 157 (2), 641-649.
38. Nelson, D. B.; Nehrir, M. H.; Gerez, V., Economic evaluation of grid-connected fuel-cell systems. Energy Conversion, IEEE Transactions on 2005**,** 20 (2), 452-458.
39. Lokurlu, A.; Grube, T.; Höhlein, B.; Stolten, D., Fuel cells for mobile and stationary applications--cost analysis for combined heat and power stations on the basis of fuel cells. International Journal of Hydrogen Energy 2003**,** 28 (7), 703-711.
40. Lipman, T. E.; Edwards, J. L.; Kammen, D. M., Fuel cell system economics: comparing the costs of generating power with stationary and motor vehicle PEM fuel cell systems. Energy Policy 2004**,** 32 (1), 101-125.
41. Adamson, K. A., Stationary fuel cells: an overview. Elsevier Science Ltd: 2007.
42. Hawkes, A.; Brett, D.; Brandon, N., Fuel cell micro-CHP techno-economics: Part 2-Model application to consider the economic and environmental impact of stack degradation. International Journal of Hydrogen Energy 2009**,** 34 (23), 9558-9569.
43. Jeong, H.; Ha, T.; Kim, H.; Han, C., Simulation of PEM fuel cell with 2D steady-state mode. Korean Chemical Engineering Research 2008, 915-921.
44. Himmelblau, D. M., Basic principles and calculations in chemical engineering. 1982.
45. Bird, R.; Stewart, W.; Lightfoot, E., Transport Phenomena. Wiley, New York 1960.
46. DOE, U., Multi-Year Research, Development and Demonstration Plan: Planned Program Activities for 2005-2015. US Department of Energy, Office of

Energy Efficiency and Renewable Energy, Hydrogen, Fuel Cells and Infrastructure Technologies Program (HFCIT) 2010, 1-34.
47. Towler, G. P.; Mann, R.; Gabaude, C. M. D., Refinery hydrogen management: cost analysis of chemically-integrated facilities. Industrial & engineering chemistry research 1996**,** 35 (7), 2378-2388.
48. Mueller-Langer, F.; Tzimas, E.; Kaltschmitt, M.; Peteves, S., Techno-economic assessment of hydrogen production processes for the hydrogen economy for the short and medium term. International Journal of Hydrogen Energy 2007**,** 32 (16), 3797-3810.
49. Balat, M., Political, economic and environmental impacts of biomass-based hydrogen. International Journal of Hydrogen Energy 2009**,** 34 (9), 3589-3603.
50. Lim, M.; Bang, J.; Yoon, Y., Analysis of hydrogen production cost by production method for comparing with economics of nuclear hydrogen. Trans. of the Korean Hydrogen and New Energy Society 2006**,** 17 (2), 218-226.
51. Cory, K. S.; Couture, T.; Kreycik, C.; Laboratory, N. R. E., Feed-in Tariff Policy: Design, Implementation, and RPS Policy Interactions. National Renewable Energy Laboratory: 2009.
52. Couture, T.; Gagnon, Y., An analysis of feed-in tariff remuneration models: Implications for renewable energy investment. Energy Policy 2010**,** 38 (2), 955-965.
53. Mansanet–Bataller, M.; Pardo, A., CO2 prices and portfolio management. International Journal of Global Energy Issues 2011**,** 35 (2), 158-177.
54. Max, S. P.; Klaus, D.; Ronald, E., Plant Design and Economics for Chemical Engineers. McGraw-Hill, Inc., USA: 2003.
55. Sundén, B.; Faghri, M., Transport phenomena in fuel cells. WIT Press: 2005.
56. Égert, B., France's Environmental Policies: Internalising Global and Local Externalities. OECD Economics Department Working Papers 2011.
57. Staffell, I., A review of small stationary fuel cell performance. 2009.
58. Wagner, M. W.; Uhrig-Homburg, M., Futures price dynamics of CO2 emission certificates—an empirical analysis. Journal of Derivatives 2009**,** 17 (2), 73-88.
59. Bartels, J. R.; Pate, M. B.; Olson, N. K., An economic survey of hydrogen production from conventional and alternative energy sources. International Journal of Hydrogen Energy 2010**,** 35 (16), 8371-8384.
60. Jeong, H.; Cho, S.; Han, C., A three-segment dynamic model simulation to predict water transport behavior in a PEMFC stack. Korean Journal of Chemical Engineering 2012, Submitted.
61. Springer, T. E.; Zawodzinski, T.; Gottesfeld, S., Polymer electrolyte fuel cell model. J. Electrochem. Soc 1991**,** 138 (8), 2334-2342.
62. Bernardi, D. M.; Verbrugge, M. W., Mathematical model of a gas diffusion electrode bonded to a polymer electrolyte. AIChE Journal 1991**,** 37 (8),

1151-1163.
63. Wang, Z.; Wang, C.; Chen, K., Two-phase flow and transport in the air cathode of proton exchange membrane fuel cells. Journal of power sources 2001**,** 94 (1), 40-50.
64. Siegel, N.; Ellis, M.; Nelson, D.; Von Spakovsky, M., Single domain PEMFC model based on agglomerate catalyst geometry. Journal of power sources 2003**,** 115 (1), 81-89.
65. Djilali, N., Computational modelling of polymer electrolyte membrane (PEM) fuel cells: Challenges and opportunities. Energy 2007**,** 32 (4), 269-280.
66. Siegel, C., Review of computational heat and mass transfer modeling in polymer-electrolyte-membrane (PEM) fuel cells. Energy 2008**,** 33 (9), 1331-1352.
67. Berg, P.; Promislow, K.; Pierre, J. S.; Stumper, J.; Wetton, B., Water management in PEM fuel cells. Journal of the Electrochemical Society 2004**,** 151, A341.
68. Eckl, R.; Zehtner, W.; Leu, C.; Wagner, U., Experimental analysis of water management in a self-humidifying polymer electrolyte fuel cell stack. Journal of power sources 2004**,** 138 (1), 137-144.
69. Tsushima, S.; Teranishi, K.; Nishida, K.; Hirai, S., Water content distribution in a polymer electrolyte membrane for advanced fuel cell system with liquid water supply. Magnetic resonance imaging 2005**,** 23 (2), 255-258.
70. Johnson, R.; Morgan, C.; Witmer, D.; Johnson, T., Performance of a proton exchange membrane fuel cell stack. International Journal of Hydrogen Energy 2001**,** 26 (8), 879-887.
71. Baschuk, J.; Li, X., Modelling of polymer electrolyte membrane fuel cells with variable degrees of water flooding. Journal of power sources 2000**,** 86 (1), 181-196.
72. Weber, A. Z.; Newman, J., Transport in polymer-electrolyte membranes. Journal of the Electrochemical Society 2003**,** 150, A1008.
73. Bao, C.; Ouyang, M.; Yi, B., Analysis of the water and thermal management in proton exchange membrane fuel cell systems. International Journal of Hydrogen Energy 2006**,** 31 (8), 1040-1057.
74. Karnik, A. Y.; Stefanopoulou, A. G.; Sun, J., Water equilibria and management using a two-volume model of a polymer electrolyte fuel cell. Journal of power sources 2007**,** 164 (2), 590-605.
75. Kim, K. H.; Lee, K. Y.; Lee, S. Y.; Cho, E. A.; Lim, T. H.; Kim, H. J.; Yoon, S. P.; Kim, S. H.; Lim, T. W.; Jang, J. H., The effects of relative humidity on the performances of PEMFC MEAs with various Nafion® ionomer contents. International Journal of Hydrogen Energy 2010**,** 35 (23), 13104-13110.
76. Larminie, J.; Dicks, A.; ., K., Fuel cell systems explained. 2003.
77. O'Hayre, R. P.; Cha, S. W.; Colella, W.; Prinz, F. B., Fuel cell fundamentals. John Wiley & Sons Hoboken, New Jersey: 2006.
78. Nørskov, J. K.; Rossmeisl, J.; Logadottir, A.; Lindqvist, L.; Kitchin, J.; Bligaard, T.; Jonsson, H., Origin of the overpotential for oxygen reduction at a

fuel-cell cathode. The Journal of Physical Chemistry B 2004**,** 108 (46), 17886-17892.
79. Kamarajugadda, S.; Mazumder, S., On the implementation of membrane models in computational fluid dynamics calculations of polymer electrolyte membrane fuel cells. Computers & Chemical Engineering 2008**,** 32 (7), 1650-1660.
80. Guzzella, L. In Control oriented modelling of fuel-cell based vehicles, 1999.
81. Gurau, V.; Liu, H.; Kakac, S., Two dimensional model for proton exchange membrane fuel cells. AIChE Journal 1998**,** 44 (11), 2410-2422.
82. Baschuk, J.; Li, X., A general formulation for a mathematical PEM fuel cell model. Journal of power sources 2005**,** 142 (1), 134-153.
83. Nguyen, P. T.; Berning, T.; Djilali, N., Computational model of a PEM fuel cell with serpentine gas flow channels. Journal of power sources 2004**,** 130 (1), 149-157.
84. Patankar, S. V., Numerical heat transfer and fluid flow. Hemisphere Pub: 1980.
85. Um, S.; Wang, C.; Chen, K., Computational fluid dynamics modeling of proton exchange membrane fuel cells. Journal of Electrochemical Society 2000**,** 147 (12), 4485-4493.
86. Moore, R.; Hauer, K.; Friedman, D.; Cunningham, J.; Badrinarayanan, P.; Ramaswamy, S.; Eggert, A., A dynamic simulation tool for hydrogen fuel cell vehicles. Journal of power sources 2005**,** 141 (2), 272-285.
87. Pukrushpan, J. T.; Stefanopoulou, A. G.; Peng, H., Control of fuel cell power systems: principles, modeling, analysis, and feedback design. Springer Verlag: 2004.
88. McKay, D.; Ott, W.; Stefanopoulou, A., Modeling, parameter identification, and validation of reactant and water dynamics for a fuel cell stack. Proceedings of IMECE 2005.
89. Jeong, H.; Cho, S.; Kim, D.; Pyun, H.; Ha, D.; Han, C.; Kang, M.; Jeong, M.; Lee, S., A heuristic method of variable selection based on principal component analysis and factor analysis for monitoring in a 300 kW MCFC power plan. International Journal of Hydrogen Energy 2012, On-line published.
90. Glauz, W. W. Molten carbonate fuel cell power plant located at termincal island wastewater treatment plant; Los Angeles Department of Water and Power (US): 2004.
91. McPhail, S. J., Status and Challenges of Molten Carbonate Fuel Cells. Advances in Science and Technology 2011**,** 72, 283-290.
92. Mangold, M.; Grötsch, M.; Sheng, M.; Kienle, A., State estimation of a molten carbonate fuel cell by an extended Kalman filter. Control and observer design for nonlinear finite and infinite dimensional systems 2005, 93-109.
93. Lee, S.-Y.; Kim, D.-H.; Lim, H.-C.; Chung, G.-Y., Mathematical modeling of a molten carbonate fuel cell (MCFC) stack. International Journal of Hydrogen Energy 2010**,** 35 (23), 13096-13103.

94. Sheng, M.; Mangold, M.; Kienle, A., A strategy for the spatial temperature control of a molten carbonate fuel cell system. Journal of power sources 2006**,** 162 (2), 1213-1219.
95. Greppi, P.; Bosio, B.; Arato, E., A steady-state simulation tool for MCFC systems suitable for on-line applications. International Journal of Hydrogen Energy 2008**,** 33 (21), 6327-6338.
96. Milewski, J.; Świercz, T.; Badyda, K.; Miller, A.; Dmowski, A.; Biczel, P., The control strategy for a molten carbonate fuel cell hybrid system. International Journal of Hydrogen Energy 2010**,** 35 (7), 2997-3000.
97. Monaco, A.; Di Matteo, U., Life cycle analysis and cost of a molten carbonate fuel cell prototype. International Journal of Hydrogen Energy 2011.
98. Rashidi, R.; Berg, P.; Dincer, I., Performance investigation of a combined MCFC system. International Journal of Hydrogen Energy 2009**,** 34 (10), 4395-4405.
99. Fermeglia, M.; Cudicio, A.; DeSimon, G.; Longo, G.; Pricl, S., Process simulation for molten carbonate fuel cells. Fuel Cells 2005**,** 5 (1), 66-79.
100. Wee, J. H., Molten carbonate fuel cell and gas turbine hybrid systems as distributed energy resources. Applied Energy 2011.
101. MacGregor, J. F.; Kourti, T., Statistical process control of multivariate processes. Control Engineering Practice 1995**,** 3 (3), 403-414.
102. Nomikos, P.; MacGregor, J. F., Multivariate SPC charts for monitoring batch processes. Technometrics 1995, 41-59.
103. Wold, S.; Esbensen, K.; Geladi, P., Principal component analysis. Chemometrics and Intelligent Laboratory Systems 1987**,** 2 (1-3), 37-52.
104. Chiang, L. H.; Russell, E. L.; Braatz, R. D., Fault diagnosis in chemical processes using Fisher discriminant analysis, discriminant partial least squares, and principal component analysis. Chemometrics and Intelligent Laboratory Systems 2000**,** 50 (2), 243-252.
105. Piovoso, M. J.; Kosanovich, K. A., Applications of Multivariate Statistical-Methods to Process Monitoring and Controller-Design. International Journal of Control 1994**,** 59 (3), 743-765.
106. Raich, A.; Ēinar, A., Multivariate statistical methods for monitoring continuous processes: assessment of discrimination power of disturbance models and diagnosis of multiple disturbances. Chemometrics and Intelligent Laboratory Systems 1995**,** 30 (1), 37-48.
107. Wise, B. M.; Gallagher, N. B., The process chemometrics approach to process monitoring and fault detection. Journal of Process Control 1996**,** 6 (6), 329-348.
108. Bozzini, B.; Maci, S.; Sgura, I.; Lo Presti, R.; Simonetti, E., Numerical modelling of MCFC cathode degradation in terms of morphological variations. International Journal of Hydrogen Energy 2011**,** 36 (16), 10403-10413.
109. Westerhuis, J. A.; Kourti, T.; MacGregor, J. F., Comparing alternative approaches for multivariate statistical analysis of batch process data. Journal of

Chemometrics 1999**,** 13 (3-4), 397-413.
110. Barbieri, P.; Adami, G.; Piselli, S.; Gemiti, F.; Reisenhofer, E., A three-way principal factor analysis for assessing the time variability of freshwaters related to a municipal water supply. Chemometrics and Intelligent Laboratory Systems 2002**,** 62 (1), 89-100.
111. Zhang, J.; Roberts, P., Process fault diagnosis with diagnostic rules based on structural decomposition. Journal of Process Control 1991**,** 1 (5), 259-269.
112. Conlin, A.; Martin, E.; Morris, A., Confidence limits for contribution plots. Journal of Chemometrics 2000**,** 14 (5-6), 725-736.
113. Weighell, M.; Martin, E.; Bachmann, M.; Morris, A.; Friend, J. In Multivariate statistical process control applied to an industrial production facility, IFAC Conference ADCEM'97, Banff, Canada Banff, Canada 1997.
114. Neyman, J.; Pearson, E. S., The testing of statistical hypotheses in relation to probabilities a priori. Joint Statistical Papers 1967, 186-202.

Abstract in Korean (요 약)

석유 고갈에 대한 우려와 환경 문제의 증가에 따라 연료 전지 기술의 가치가 높게 평가 받고 있다. 화학 공단에서 생산되는 부생 수소는 다른 화학 공정이나 정유 공정에서 사용되거나 보일러의 연료로 쓰이고 있다. 부생 수소를 좀더 효율적으로 사용하는 기술에 대한 필요성이 대두되고 있는 상황에서 수소를 고효율로 사용할 수 있는 연료 전지 기술이 상용화 수준으로 발전하고 있다. 본 논문에서는 고분자 전해질 연료 전지 (Proton Exchange Membrane Fuel Cell: PEMFC) 발전소의 경제성 분석, PEMFC의 이동 현상 분석, 용융 탄산염 연료 전지 (Molten Carbonate Fuel Cell: MCFC) 발전소를 위한 감시 시스템의 개선이라는 세 가지 주요 목표를 담고 있다.

부생 수소를 사용하는 방법의 하나로 PEMFC 발전소의 경제성을 분석하였다. 이를 위해 연료 전지 발전소의 경제적 타당성을 검증하기 위한 공정 모델을 개발하였다. 또한, 경제적 타당성의 기준으로 현재의 상황에 대한 경제성 분석과 중요 변수에 대한 민감도 분석을 수행하였다. 미래의 상황을 감안하기 위해서 정부 지원 제도 변화와 수소 가격의 변화를 고려하였다. 다양한 수소 생산 방식을 비교한 결과 화학 공단에서 생산되는 부생 수소를 사용한 경우가 경제적 이점을 가지고 있음을 확인하였다.

본 논문에서는 단위 전지와 스택에서 일어나는 이동 현상을 모사하기

위해서 정적 모델과 동적 모델을 사용하였다. PEMFC 단위 전지의 모사를 위해서는 2차원의 정적 상세 모델을 개발하였다. 모델을 이용하여 가스의 이동, 전기화학 반응, 전류 분포와 유체 역학에 대한 계산을 수행하였다. 지배 방정식들은 유한 체적법에 기초한 유체 역학 계산 알고리즘을 이용하여 계산하였다. 제안된 방법은 실험을 통해 얻은 분극 곡선과의 비교를 통해 검증하였다. PEMFC 스택의 모사를 위해서는 무차원의 동적 모델을 개발하였다. 성능과 물 관리 사이의 보다 정확한 관계를 규명하기 위하여 일괄 모델 (Lumped model)을 수정한 동적 모델을 사용하였다. 이 둘 사이의 관계를 분석하기 위해서 수정된 모델은 입구단, 중앙단, 출구단의 세 부분으로 구성하였다. 전해질 막을 통과하는 물의 양과 각 단에서의 전류 변화를 계산하였다. 모사 결과는 일괄 스택 모델의 결과와 참고 문헌의 비교를 통해 분석하였다. 물 공급이 원활하지 않은 운송용 연료 전지에서는 출구단에서의 물 양이 중요하기 때문에 물 양의 예측은 연료 전지 자동차에서 중요한 역할을 차지한다.

300kW급 MCFC 발전소에서는 상한 값과 하한 값 기준만을 가지고 있는 단변수 알람 시스템이 일반적으로 적용되어 있다. 이러한 단순한 감시 시스템은 이상 진단을 위한 모니터링 시스템 확장에는 한계점을 가지고 있다. 따라서 주성분 분석 (Principal Component Analysis: PCA)에 기반한 다변량 감시 시스템을 위해 경험적 변수 선정 방법을 개발하였다. 실제 운전 데이터를 이용하여 이상 감지의 성능을

검증하였다. I 형과 II 형 에러율을 비교한 결과 네 가지 변수 그룹에서 경험적 방법론이 이상이 일어남을 잘 감지함을 검증할 수 있었다. 이러한 감시 기술은 현장에 설치되어 있는 MCFC 발전소에서 정상 상태와 이상 상태를 구별하지 못하여 울리는 잘못된 알람을 줄이는 데 사용할 수 있다.

다양한 경우에 대한 모델링과 모사에 관한 연구 결과들은 모사의 여러 목적에 맞게 적합한 모델링 방법을 선정하는 데 이용될 수 있을 것이다. 또한, 제안된 모델들은 효율적인 디자인과 안정적인 운전과 같은 다른 목적을 위해 사용될 수 있을 것이다.

주요어: 연료전지, 모델링과 시뮬레이션, 이동 현상, 공정 감시, 경제성 분석

학번: 2006-21388
성명: 정현석